

University of Verona Science and Technology Department, Italy

Report for CEEP BIT (Comité Européen d'Etudes des Polyphosphates) a CEFIC Sector Group, Dec. 2002

Study of operating results and process optimisation of the struvite crystallisation process at the Treviso municipal waste water treatment plant (wwtp).

Abstract

The work summarizes the activities made on the SCP reactor during a first period of observations. First of all there is an introduction concerning the Italian situation concerning existing treatment plants which operate the biological nutrient removal. P removal is always associated with phosphorus release and the work shows the existing way to remove it with the precipitation process that guarantees the possibility of recycling and reusing. Several models are available in literature to describe the phosphorus precipitation process. In the Treviso Waste water treatment plant phosphorus removal from supernatants is realized with the precipitation of MAP or HAP in a fluidized bed reactor filled with silica sand: precipitation conditions are gained simply with increase of pH in the supernatants made by air supply.

Several tests are requested before running with the precipitation tests. They are necessary to investigate the supernatants natural behaviour with time and the possibility of MAP or HAP precipitation as a consequence of supersaturation condition. They show that supernatant reach supersaturation condition in several days and that it is possible to precipitate MAP or HAP depending on initial conditions of the supernatants. When P content is low, the calcite can precipitate with MAP, but when P concentration in supernatant increases, HAP is the predominant salt.

Other tests (Hydraulic tests Air stripping tests) are used to control the hydraulic behaviour of the demonstrative plant, to define the value of the air flow rate necessary to reach the desired pH value in the supernatant entering the plant.

Precipitation tests, summarised in this report, take place from April 2001 to July 2002. They are made with different conditions of P content in supernatants, of air flow rate, inner flowrate and contact time. They are discussed in terms of removal efficiency even if further investigations will prove if the obtained results correspond with the theoretical-experimental model deduced from previous experimentation on pilot plants. Analysis on silica sand are made to prove the growth of the bed (sieve analysis of sand particle, bed porosity) and to control the precipitated salt on the sand particles (chemical analysis of the bed). During the period studied the expansion tank in the upper section of the fluidised bed reactor was substituted with a larger one so to avoid the outgoing of fine sand particles and the exhaust sand was replaced. This was due to the deposition of organic materials, coming in the plant with the solids of the supernatants, that make dirty the surface of sand grain and prevent the deposition of P-salt.

Future tasks include further precipitation tests and the study of the mathematical model with the SCP results. To prevent the incoming of organic solids a new apparatus will be designed and applied.

1 Introduction and state of the art

Phosphorus recovery in civil wastewater treatment plants is mainly achieved treating the supernatants coming from the sludge anaerobic digestion section. To reach high contents of orthophosphates in this stream, the biological nutrient removal must be applied in the wastewater treatment line, which has to be planned considering that P release has to be carried out in a controlled way in one single point of the process, in order to have small streams rich in phosphorus to treat. This scenery is typical for Europe, North America and South Africa as well, but not for Italy, mainly because of the low P content in sewerage networks and of the low content in readily biodegradable carbon sources (RBCOD) in the wastewater to be treated.

The situation in Italy concerning the existing wastewater treatment plants which are actually running on a nutrient removal basis can be evaluated starting from a national analysis carried out in 1996, considering 13 regions on 20 and the plants with a capacity larger than 50.000 P.E.

In particular, over 157 plants considered, 77% use the primary settling option, while the other 23% doesn't use this approach. The 52% can reach an effective N removal, even if the process schemes consider only nitrification (N, 27%) or predenitrification-nitrification (DN, 66%), and 7% runs on a BNR process basis. In other words, only 6 plants are running as BNR in the whole country, even though this fraction is continuously increasing following the EC directive 271/91. The leading processes among the existing BNR plants are the A2O and the Phostrip configurations.

The optimisation of a process for phosphorus recovery from civil wastewater is linked to the evaluation of the real problems concerning the management of the biological nutrient removal (BNR) process.

In BNR plants phosphorus is released in the anaerobic step and when an adequate concentration of VFA or, more generally, RBCOD is present. The rate of release is linked to:

- the treatment scheme,
- the operational conditions of each unit operation;
- the inlet physical-chemical characteristics.

The phenomenon is always massive, and it can be equal to the P removed in water line. It is present mainly in sludge line, thus an adequate treatment of the sludge or at least of the supernatants, before the recycle to the headworks, has to be done.

The planning strategy of the sludge line should pursue the double aim of restraining the release process and concentrating it in a single point of the line for the definitive removal. This can be obtained using a process scheme in which the waste activated sludge (WAS) is thickened separately from the primary ones (PS). Then, they can be treated to avoid the release in supernatants (e.g. composting, landfill, incineration) or to increase it (i.e. anaerobically) in a way to concentrate the phosphorous in the supernatants and thus leading to a lower flow to treat (Randall et al.; 1992).

Table 1 - Phosphorus release in primary sedimentation and sludge thickening

WWTP	Process	Unit operation	P released, (%)	P, (mg/l)	Reference
A	BNR	WAS thickening	4	20	Randal et al., 1992
A ₁	BNR	WAS thickening	22	12	Randal et al., 1992
B	BNR	Mixed primary sedimentation	43		Randal et al., 1992
C	BNR	WAS +PS thickening	42	60-100	Murakami et al., 1987
D	BNR	WAS thickening	1.9	9.8	Tanaka et al., 1987
D ₁	BNR	WAS + PS thickening (1/1)	37	64-131	Tanaka et al., 1987
D ₂	BNR	WAS + PS thickening (2/1)	34	64-131	Tanaka et al., 1987

This approach is linked to the fact that the primary sludge are a good source of carbon, which can be used for the phosphorus release step; thus both settling and gravitational thickening of the mixed sludge should be avoided in a BNR approach. Evidences in this field came from the monitoring of full scale plants (Tab.1) in which WAS gravitational thickening in short times (HRT=10-25 h) lead to phosphorus small release (2-4%, examples A and D in Tab.1), while settling and thickening of mixed sludge showed releases in the order of 40% (examples A₁, B, C, D₁, and D₂ – Tab.1).

In the anaerobic digestion process phosphorus release is mainly due to the high concentration of VFA, which is typical of this process. Moreover, biologically active ions, such as potassium (K) and magnesium (Mg), which play a major role in the stabilisation of the intracellular polyphosphates negative charge, are widely released. This release follows the molar ratios, which range from 0.3 mol K/mol P to 0.26 mol Mg/mol P (Popel and Jardin, 1993; Wentzel et al., 1992).

The total amount of phosphorus released in the digester can be different from the amount actually recycled to headworks, since re-precipitation processes may take place. Thus, the maximum observed release in conventional plants is up to 20%, while it may reach 43-63 % in BNR plants with medium-high P content in the sludge. It can be raise up to 95% in plants in which sludge P content is 7%TS.

The real released amount observed in full-scale plants shows values which can widely differ one from each other; this can be ascribed to:

- the hardness of the inlet, because it controls the re-precipitation processes of phosphorous inside the digester;
- the ratio of supernatant flow rates to the inlet, which can change a lot using pre-thickening of sludge before digestion.

Re-precipitation can occur mainly as struvite (MAP: MgNH_4PO_4) or hydroxyapatite (HAP: $\text{Ca}_5\text{OH}(\text{PO}_3)_3$). Other forms of minerals are hypothesized, such as vivianite ($\text{Fe}_2(\text{PO}_4)_3 \cdot 8\text{H}_2\text{O}$) and bruscite ($\text{Ca HPO}_4 \cdot 2\text{H}_2\text{O}$) (Nancollas, 1984). Struvite precipitation, which is thermodynamically less advantageous than Hydroxylapatite ($K_{ps}=12.6$ vs 57.8 respectively), is kinetically promoted by the high pH of the supernatant (7.4 – 7.9) and by the inhibition exerted by alkalinity on hydroxylapatite crystallisation (Jenkins et al., 1971).

Phosphate removal from supernatants or from the main streams leading to the production of a recyclable material in the form of phosphate pellets should be desirable; in particular, in case pellets with a low water content and a relatively high P content are obtained, they can be used either as a slow release fertiliser or as other industrial products (e.g. cleaning products, chemicals, fire retardants). In this way the costs of phosphorus removal could be balanced by the gain of a recyclable phosphate product and by the reduction of sludge disposal costs, due to less sludge amount and volume. However, it is necessary to keep the formation of very small particles (i.e. fines) under control, as these cannot be recovered and/or can generate a non-manageable sludge that would make the plant configuration more complex.

Key issues in reactor design parameters for phosphate precipitation are thus kinetics (ensuring mixing but avoiding abrasion) and flowrates (which define reactor size and consequently costs). The objectives are to obtain a reasonably high level (about 80-90%) of phosphate removal from the solution by precipitation and to establish reactor designs which offer simplicity, robustness and low costs compatible with wastewater treatment plant operation. Moreover it is essential to define how operating parameters can be adapted to specific plant conditions, in particular suspended solids, by varying the concentrations of phosphate and other components and varying the temperature and to establish the reliable production of a reusable product.

Among the different processes devised to extract phosphorus from wastewater prior to crystallization in a dedicated reactor, we can mention (Stratful et al., 1999): the DHV CrystalactorTM, the Rim-Nut ion exchange process, the Unitika Phosnix process and the Kurita fixed bed crystallization.

The DHV CrystalactorTM system (Eggers et al., 1991) consists of a cascade degassifier, a fluidized bed reactor and two pressure filters. The process is based on a fluidized reactor, in which calcium phosphate crystallizes on a seeding grain, typically sand. During the operation, pellets increase in diameter, and are removed and replaced by smaller ones once they have reached the desired size. Some amorphous phosphate is lost in a suspended form (carry-over), therefore a dual media filtration is required, with additional capital and operational costs. The RIM-NUT ion exchange precipitation process (Liberti et al., 1986) removes phosphate and ammonia ions from tertiary wastewater producing ammonium phosphate (struvite, NH_4MgPO_4). The process consists of three stages (two columns of cationic resin, two column of anionic resin and the nutrient precipitation process). A dual column system is adopted for each resin to allow regeneration simultaneously with nutrient removal. The Phosnix process (Unitika Ltd., 1994) is a side stream process, and treats phosphorus enriched wastewater (e.g. effluent from digesters, fermenters, biological nutrient removal systems). Digester effluent is fed into the base of the tower where it is mixed with magnesium chloride. Caustic soda is dosed to ensure a pH in the range 8.5-9, thus the conditions for spontaneous nucleation and growth of struvite crystals are obtained. The Kurita fixed bed crystallization column (Joko, 1984) is based on similar chemistry to the DHV CrystalactorTM. The equipment consists in a fixed bed column reactor, packed with phosphate rock seeding grains.

Secondary effluent is fed into the base of the column and travels upwards through the column. The phosphate depleted effluents leave the top of the column.

All the above mentioned techniques are worthy, but need the addition of chemical species to adjust the experimental conditions, in order to allow the precipitation of phosphate salts. This research group has devised a phosphate removal technique by exclusively using the chemical physical properties of anaerobic supernatants without any addition of chemicals, reaching the operational pH only by aeration, and obtaining a quantitative removal of phosphate through nucleation on sand quartz by CO₂ stripping with air (Cecchi et al., 1994; Battistoni et al., 1996; Battistoni et al., 1997). The crystallization of phosphorus salts like hydroxyapatite (Ca₅(PO₄)₃OH - HAP) and/or struvite (MAP) has been studied in a fluidized bed reactors (FBR) on a bench scale (Battistoni et al., 1998a; Battistoni et al., 2000), and on semi scale pilot plant (Battistoni et al., 2001). Furthermore, the efficiency of the process was related to the pH and sand contact time. A double saturational model was used to describe nucleation and conversion processes.

Several models are available in literature to describe the phosphorus precipitation process; they can be distinguished by:

- models based on primary nucleation mechanism (e.g. nucleation is caused by pure supersaturation);
- models based on secondary nucleation mechanisms (e.g. nucleation and growth take place on pre-existent seeds, in metastable supersaturation conditions).

The work of Seckler et al. (1996 a,b,c) belongs to the first group, proposing a theoretical model for fine particle aggregation with sand grains. The following equation derives from a particle number balance, and expresses the decrease in the fines concentration by aggregation with grains in a fluidised bed:

$$\frac{dN_i}{dt} = -BJ_{ii}\beta$$

where B is the collision efficiency, N is the initial particle concentration, J_{ii} is the collision frequency, β is the supersaturation and t is the reaction time, which is expressed by:

$$t = \frac{\varepsilon x}{v_{sup}}$$

where ε is the bed porosity, x is the axial position and v_{sup} is the superficial velocity. The supersaturation is defined as:

$$\beta = \frac{1}{5} \ln \frac{(Ca^{2+})^3 \cdot (PO_4^{3-})^2}{K_{SP}}$$

where K_{SP} is the solubility product of amorphous calcium phosphate.

The collision efficiency B is derived from the following expression, which describes the influence of the energy dissipation rate (E):

$$B = B_0 \left(\frac{E}{E_0} \right)^\alpha$$

where E₀ is a reference value and B₀ and α are characteristic parameters of the precipitating system.

By integrating Eq.1 from $t=0$ to $t=t_{out}$, the phosphate removal efficiency η_{ag} (by aggregation only) can be calculated, by assuming the particle size of the fines to be constant in time:

$$\eta_{ag} = \frac{N_{i,in} - N_{i,out}}{N_{i,in}}$$

It was found, both theoretically and experimentally, that the aggregation can be increased by spreading the supersaturation more evenly throughout the reactor, while the breakage can be reduced by choosing fluidisation conditions where the energy dissipation rate in the bed is minimised.

Concerning the models based on secondary nucleation mechanism, De Rooij et al. (1984) studied the formation of different phases of calcium phosphates on a seed material, in well defined experimental conditions, such as a fixed value of temperature ($T=37^{\circ}\text{C}$), ionic strength ($I=0.10$ mol/l), Ca/P ratio ($\text{Ca/P}=1.333$) and for various pH values ($5 < \text{pH} < 8$). The model obtained is that showed by the following equation:

$$\frac{dm}{dt} = ks(IP^{1/v} - K_{SP}^{1/v})^p$$

where m is the number of precipitated moles, k is the rate constant for crystallisation, s a factor proportional to the number of sites available for growth, p the effective order of reaction, v the number of ions in the formula unit, IP the ionic product of supersaturated solution and K_{SP} the thermodynamic solubility product. The Gibbs free energy related to the transfer from supersaturated solution to an assumed saturated solution at the surface of the developing solid phase, gives the relationship between IP and K_{so} (De Rooij et al., 1984).

Kaneko and Nakajima (1988), in order to describe the crystal growth of HAP, starting from a metastability condition of synthetic water solutions in which the dependence of pH is not present, give an approximation of Eq. (7) expressed as:

$$\frac{dC}{dt} = ksC^2$$

where C is the molar concentration and t is the retention time.

Since it was demonstrated that for the crystallisation of MAP and HAP from the anaerobic supernatant in fixed bed reactors FBR works in conditions of metastability (Battistoni et al., 1998b), the approximation made by Kaneko and Nakajima (1988) is appropriate. This kinetic equation can be integrated from 0 to t , leading to the empirical saturational model in the contact time (t_c) (Eq. 8) of crystallisation efficiency η (Battistoni et al., 2000):

$$\eta = E_m \frac{t_c}{t_{1/2} + t_c}$$

Moreover, the maximum crystallisation efficiency (E_m) and the half time ($t_{1/2}$) can be introduced:

$$E_m = \frac{C_0 - C_t}{C_0}$$

$$t_{1/2} = \frac{1}{(C_0 - C_t) \cdot k}$$

where C_t is the final concentration and C_0 the initial concentration.

2. Materials and methods

2.1 Natural ageing tests

The chemical transformations with time and the behaviour of an anaerobic supernatant with natural CO_2 production was observed during the cooling of digestion sludge in an open lagoon (Salutsky et al., 1972). Following studies were done to analyse phosphorus removal, (Battistoni et al., 1997; Battistoni et al., 1998b) in order to investigate the behaviour of the system in natural conditions and the way to increase the P-removal process (nucleation and/or precipitation).

The simple methodology consists in the following procedure.

Put 5 litres of supernatant enriched with the appropriate amount of phosphorous in an open container with a good superficial exposition and left aside in a thermostatic room (25°C). Daily sample are withdrawn and the following parameter are analysed:

- pH
- P- PO_4 tot
- P- PO_4 sol
- alkalinity
- Ca
- Mg
- K^1

The test could be carried out both in the natural supernatants and in the supernatant enriched with NH_4 et PO_4 .

- The soluble P- PO_4 is analysed on 0.45 μm filtrate sample then acidified with sulphuric acid at pH 5.
- The total P- PO_4 (soluble+particles) is analysed in acidified sample (pH 5 with sulphuric acid), then, after one hour, the sample is filtered and analyzed.
- The analyses of the concentration of Ca et Mg et K are carried out in the acidified and filtered sample.

All the analyses were carried out in accordance with Standard Methods (APHA, 1982) and CNR-IRSA (1985).

2.2 Supersaturation test

The supersaturation curves are utilised to highlight the inhibition effect of ions in anaerobic liquors on struvite (MAP) and hydroxyapatite (HAP) formation. The curves were introduced by Joko (1984) and are based on phosphate addition (as Na_3PO_4 or H_3PO_4) and pH increase by adding alkali and by aeration. The supernatant could be Ca- or Mg- enriched to investigate their inhibition effect on MAP or HAP formation. In the same way it is possible to proceed with NH_3 or alkali addition. At each different P concentration, the pH value, in which supersaturation condition is verified, is obtained. The Joko methodology was modified by monitoring the solution transmittance at 400 nm and the critical supersaturation point is determined when the transmittance value reached 80% (equivalent to a turbidity of 100-170 SiO_2 mg/l).

In this way for each P concentration value it is possible to obtain the pH value that promote crystallization.

¹ Potassium could be measured only at the beginning of the test.

2.3 Wastewater chemical analyses

Outlet and inlet samples were withdrawn to analyse the following parameters:

- P-PO₄ sol
 - P-PO₄ tot
 - N-NH₄
 - TSS
 - Ca
 - Mg
 - K
 - PH
 - Alkalinity
- The soluble P-PO₄ is analysed on 0.45 µm filtrated sample then acidified with sulphuric acid at pH 5. The analyse is done by the use of a high performance liquid chromatography (HPLC MOD.DX120) using conductivity detector.
 - The total P-PO₄ (soluble + particles) is analysed in acidified sample (pH 5 with sulphuric acid), then, after one hour, the sample is filtered and analysed. The analyse is done by the use of a high performance liquid chromatography (HPLC MOD.DX120) using conductivity detector.
 - The analyses of the concentration of Ca et Mg et K were carried out in the acidified and filtered sample. The analyses were done by a high performance liquid chromatography (HPLC MOD.DX120) using conductivity detector.
 - The analysis of ammonia concentration was carried out according to the Nesslerization methods. The sample absorbance was measured at 410 nm with a spectrophotometer, after a preliminary distillation step.

All the analyses were carried out in accordance to the Standard Methods (Apha, 1982) and CNR-IRSA (1985).

2.4 Silica chemical analysis

For the determination of the main anions (phosphates) and cations (potassium, magnesium and calcium) in silica granules, the sample must be brought to solution. The analysis is done by the use of a high performance liquid chromatography (HPLC MOD.DX120) using a conductivity detector. The pre-treatment of the sample is done acidifying 2 mg of silica by adding 10 ml of hydrochloric acid .

The solution is then warmed up to 80-90°C for about 30 minutes. The cooled and filtered sample is then diluted to 250 ml with distilled water.

The samples now must be diluted (1/10 for anions and 1/5 for cations) and then are ready to be injected in the HPLC.

2.5 Sieve analysis of sand particles. Granulometric analysis on silica

The granulometric distribution test is carried out in accordance with ASTM .

This parameter is commonly determined by sieving a representative sample through a set of calibrated sieves (Table 2 reports 6 different meshes sieves used in the specific test). The vertical stack of successively finer sieves to the pan at the bottom is shaken then the amount of sand held between adjacent sieves is weighted. With simple calculations it is possible to determine the percentage of passing through materials. Starting with the weight of sieving shaken through a vertical

stack of successively fines sieves to the pan at the bottom, the portions of sand held between adjacent sieves are added in sequence, and the accumulative weights are recorded.

Table 2: utilized sieves for granulometric analyses

sieves	
Sieve name	Holes size, mm
500	0,5
355	0,355
300	0,3
212	0,212
180	0,18
125	0,125
90	0,09
75	0,075
bottom	

Calculation:

$$\% \text{ solid partly accumulated}_i = \frac{g_{\text{materialson sieve}_i}}{g_{\text{totalmaterial}}} \cdot 100$$

From the amount of solids partly accumulated in the previous sieves it is possible to estimate the percentage of accumulated material in the i^{th} sieve:

$$\% \text{ solids accumulated (i)} = \sum_0^i \% \text{ solids partly accumulated}_i$$

By the following equation the percentage of non accumulated material can be obtained:

$$\% \text{ passing through materials} = 100 - \% \text{ solids accumulated}_i$$

From the amount of the accumulated materials in each sieve the granulometric distribution curve can be obtained.

2.6 Bed porosity

Bed porosity is the ratio between the volume of empties and the total bed volume. This is a laboratory test.

The expression of bed porosity is the following:

$$\varepsilon = \frac{V_{\text{EXP}} - (V_{\text{SP}} M)}{V_{\text{EXP}}}$$

where: V_{EXP} is the bed total volume, V_{SP} the loaded silica specific volume and M the mass of loaded silica.

The unknown and variable term of equation during every single test is the specific volume. This term was determined according to the following methodology, at the end of each crystallisation test.

Silica samples withdrawn from the bed were mixed; 10 g of silica were weighed. Silica was placed in a 100 ml glass flask filled up with distilled water. The flask weight was known.

When the silica was inserted into the flask, the level lifted up and the water supernatant was withdrawn by a pipette until the upper level returned to the initial value. Then the flask was weighed and the difference between the weights with and without silica represented the mass of “displaced” water. The displaced volume was derived from water specific gravity (1g/ml): this was the silica volume.

For each examined silica bed we made four porosity tests and the average represented the final volume.

2.7 V'10 Test

The V'10 test was done sampling the effluent from different heights of the fluidised bed reactor. The test was used to determine the bed fluidity. The procedure consisted in placing 1 litre of sample in an Imhoff cone for 10 minutes settling. The volume of settleable solids in the cone as millilitres per litre was recorded. The volume of fluidised silica was estimated from both the concentration of solids in 1 L (g/L) and the total mass of silica in the bed. In this way it was possible to know if there was compact silica in the bed bottom and if it was necessary to increase the recycling flowrate.

This test was carried out with sample withdrawn from different heights of the fluidised bed reactor and the difference between the values at the various heights gave some information about the uniformity of the bed.

2.8 Demonstrative area of struvite

The Struvite demonstrative area was planned on the basis of the tests carried out by the University of Ancona with small and medium scale pilot plants. It can be used as a full scale device, but at the same time it is equipped with all the probes and facilities typically used in a bench scale reactor. This allows for the rapid change of operational conditions as well as for the acquisition of all the data needed in a scientific experiment. The plant is mainly composed of three sections (Fig.1):

- pre-treatment;
- stripping;
- FBR.

The pre-treatment section is composed by a mixing tank, a decanter and a stocking tank. Anaerobic supernatants are supplied to the mixer from the dewatering section (belt press; see Figure 2) by two centrifugal pumps placed in the dewatering section stocking tank. Anaerobic supernatants could be phosphate enriched, adding P-PO₄ directly in the mixer.

The liquor passes from the mixer to the decanter, where settleable solid are excluded. From the top section the liquid passes in the stocking tank through weir edges. Two Mohno pumps (P2) provide feeding for the stripping tank (Qin).

Figure 1 - Demonstrative area of struvite crystallization in Treviso WWTP

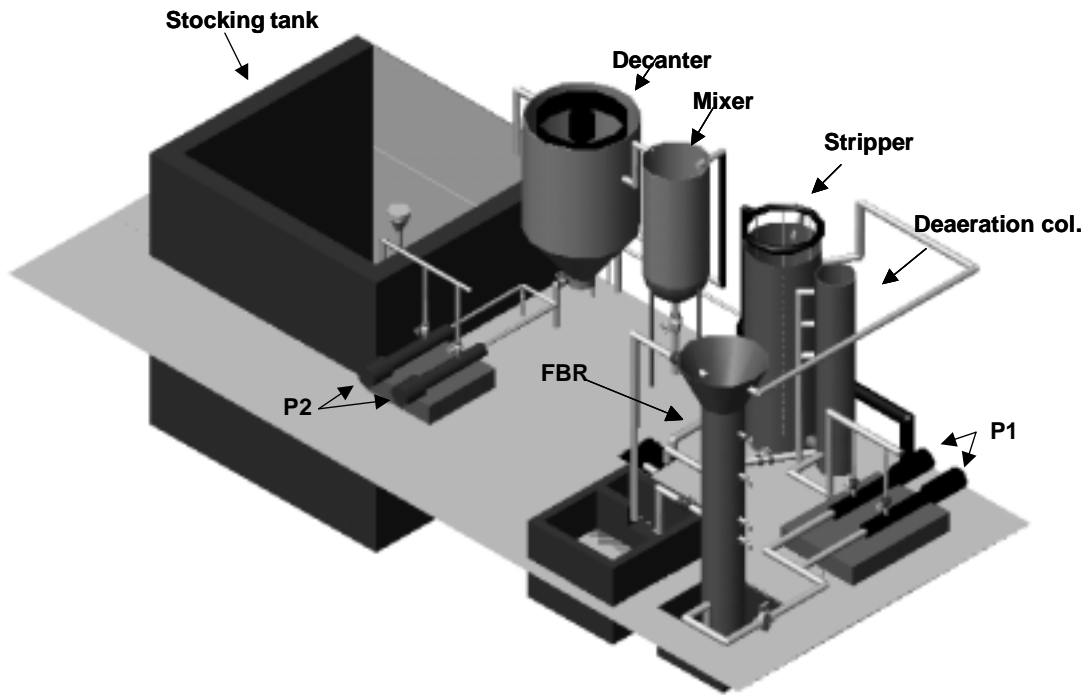
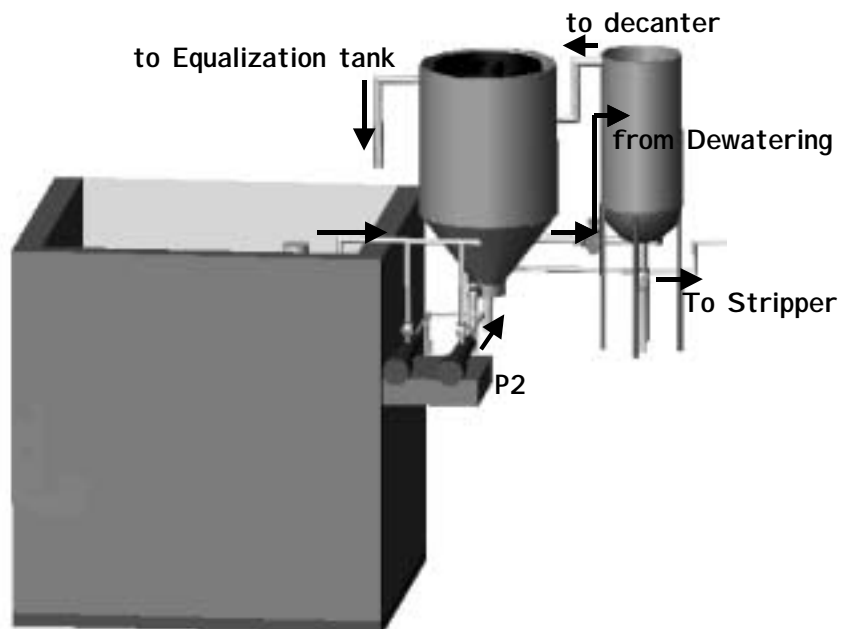


Figure 2 - stocking tank

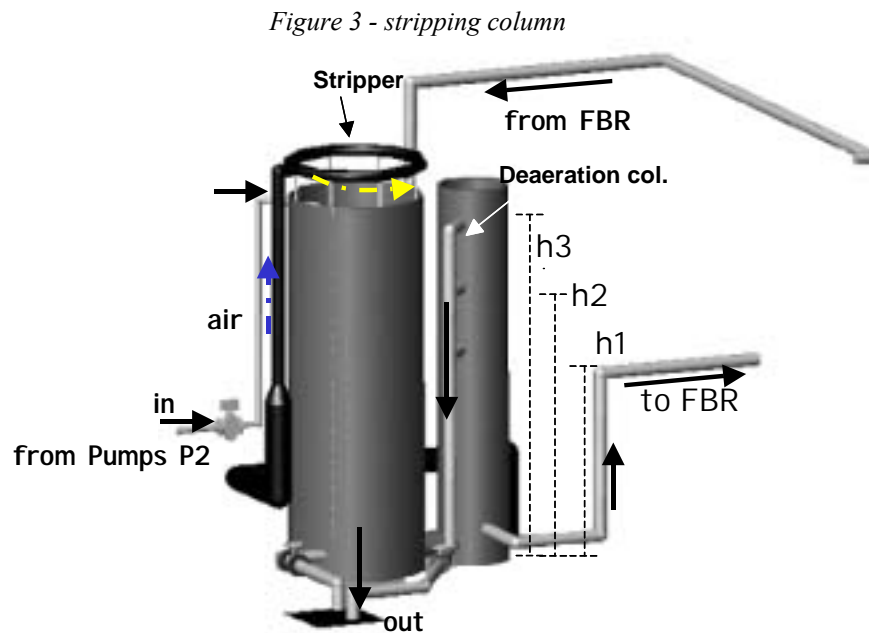


In Table 3 the volume and the electromechanical characteristics of the pre-treatment section are presented.

Table 3 - Characteristics of the pre-treatment section

Section	Materials and characteristic	Volume, geometry and flowrate
Mixer	Cylindrical steel tank	$\Phi = 0.9 \text{ m}$, $V_{\text{tot}} = 1.3 \text{ m}^3$
Decanter	Cylindrical steel tank	$\Phi = 1.6 \text{ m}$, $V_{\text{tot}} = 4.7 \text{ m}^3$
Stocking tank	Reinforced concrete tank	$V_{\text{tot}} = 48 \text{ m}^3$
Pumps P2	Mohno pump (1.5 kW)	$0.8 - 4.9 \text{ m}^3/\text{h}$

The supernatant flows from the stocking tank to the stripper, through a pump (P2, Fig.3); furthermore the liquid (recycle flowrate, Q_r) comes out from the stripper towards the fluidised bed reactor (FBR).



In the stripper tank an air diffuser is used for a flowrate up to 50 L/min.

At the stripper bottom there is a valve for cleaning the tank; moreover the de-aeration column is connected to the stripper by an horizontal pipe.

The liquid flows from the de-aeration column to the FBR through pump P1.

The column has three outlets at three different heights (h_1 - h_2 - h_3): in line with the height it is possible to set up different volumes and then different operational conditions (i.e. retention times).

In table 4 the volume and the electromechanical characteristics of the stripper are presented.

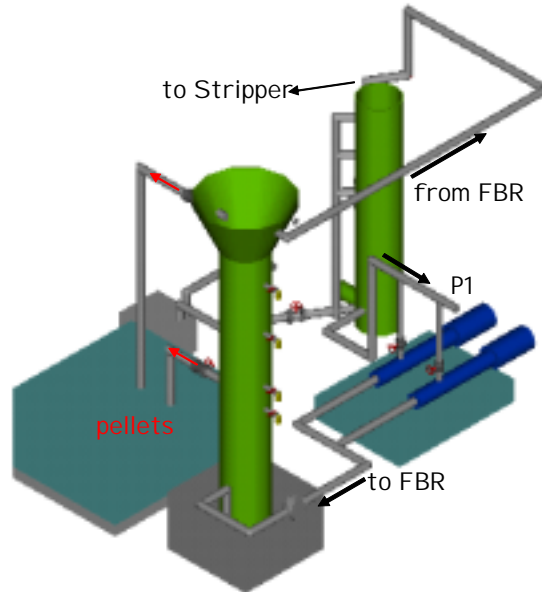
Table 4 - Characteristics of the stripping section

Section	Materials e characteristics	Volume, geometry , flowrate
Stripper	Cylindrical steel tank	$\Phi = 1 \text{ m}$,
		$H_1 = 1.7 \text{ m}$ $V_{\text{tot}} = 1.33 \text{ m}^3$
		$H_1 = 2.2 \text{ m}$ $V_{\text{tot}} = 1.73 \text{ m}^3$
		$H_1 = 2.7 \text{ m}$ $V_{\text{tot}} = 2.12 \text{ m}^3$
De-aeration column	Cylindrical steel tank	$\Phi = 0.5 \text{ m}$,
		$H_1 = 1.7 \text{ m}$ $V_{\text{tot}} = 0.33 \text{ m}^3$
		$H_1 = 2.2 \text{ m}$ $V_{\text{tot}} = 0.43 \text{ m}^3$
		$H_1 = 2.7 \text{ m}$ $V_{\text{tot}} = 0.53 \text{ m}^3$

The supernatant passes through the Mohno pumps P1 from the de-aeration column to the bottom of the FBR; here there is a gravel filter to avoid sand backflow in the pumps P1.

The FBR reactor (Fig.4) is a cylindrical steel tank with a Dortmund at the top to avoid sand wash-out. The column is filled up with sand to make half the reactor a highly compressed bed. Samples are taken from sampling ports positioned at different heights.

Figure 4 – Scheme of the FBR reactor



Silica pellets, enriched in HAP and/or MAP, go out through two pipes, one at the top of the column and one at the bottom. The liquid from the FBR goes back to the stripper through an horizontal pipe. This flow is called recycle flowrate (Q_r).

The main geometrical characteristic of the FBR reactor are represented in table 5.

Table 5 - Main characteristic of the FBR reactor

Section	Material and characteristics	Volume, geometrical and flowrate
FBR reactor (expanded bed)	Cylindrical steel tank	$\Phi = 0.6 \text{ m}$, $H = 3 \text{ m}$, $V_{\text{tot}} = 0.85 \text{ m}^3$
FBR reactor (gravel filter)	Cylindrical steel tank	$\Phi = 0.6 \text{ m}$, $H = 1 \text{ m}$, $V_{\text{tot}} = 0.28 \text{ m}^3$
Dortmund	Steel Dortmund	$\Phi_1 = 0.6 \text{ m}$, $\Phi_2 = 1.2 \text{ m}$, $H = 0.4 \text{ m}$, $V_{\text{tot}} = 0.28 \text{ m}^3$

2.9 *Monitoring and signals acquisition*

The plant is endowed with different flowrate measure transmitters. In particular the following streams are controlled:

- inlet flowrate (electromagnetic measurer ABB Kent-Taylor 4-20 mA; the flowrate from stoking tank to the stripper that is the real volume of treated supernatant is calculated);
- air flowrate;
- recycle flowrate (electromagnetic measurer ABB Kent-Taylor 4-20 mA; the flowrate from the de-aeration column to the FBR is calculated);
- raising flowrate (electromagnetic measurer ABB Kent-Taylor 4-20 mA; the flowrate from the dewatering section to the mixing tank is calculated);

The plant is also endowed with temperature recorders; in particular:

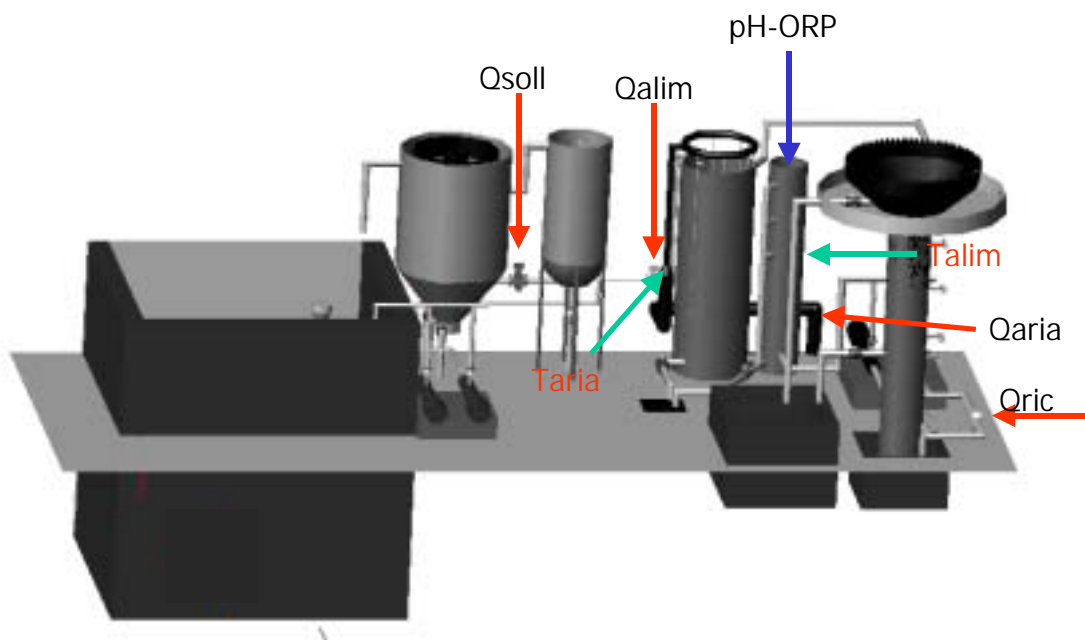
- air temperature: electronic temperature transmitter PT 100, 4-20 mA; the temperature of the air blown in the stripper is recorded;
- inlet temperature transmitter: PT 100, 4-20mA measurer

The plant is also endowed with pH and ORP measurer apparatus:

- pH (Endress+Hauser; it has been designed for continuous monitoring and control of pH, it has been placed in the de-aeration column);
- ORP transmitter (Endress+Hauser; the Redox value in the de-aeration column is measured).

All the signals are acquired and registered by a Memo-graph (Endress+Hauser).
Figure 5 shows the locations of the recording and measuring devices.

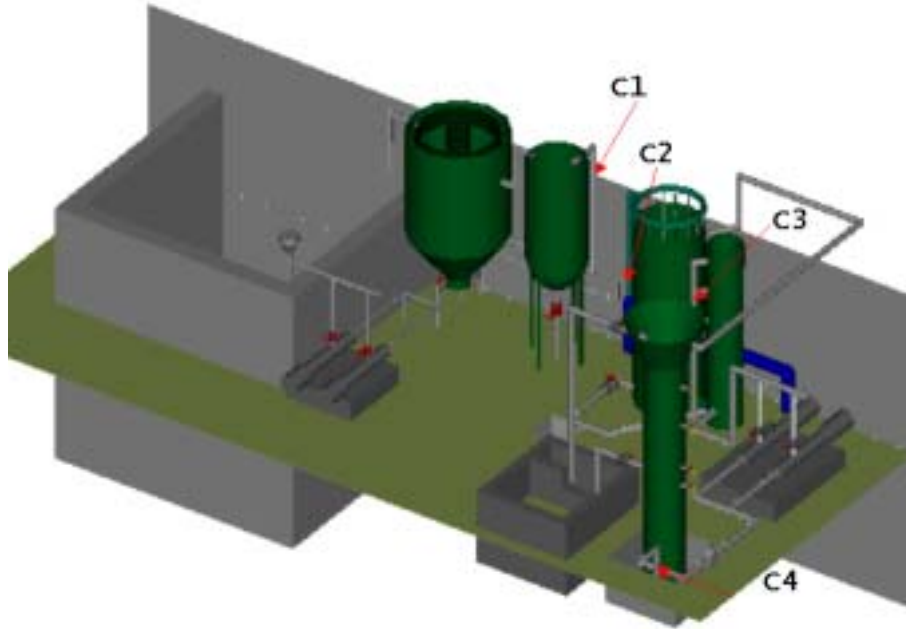
Figure 5 – Location of measuring and recording devices



2.10 Collection of samples

The plant is provided with sample withdrawal sites. Figure 6 shows the place where the automatic samplers (C1-C2-C3) have been installed to obtain average values.

Figure 6 – Sampling sites



The first sample (C1) is withdrawn from the mixer: this is the anaerobic liquor supplied from the belt press. Another sample (C2), is withdrawn from the stripper and it represents the real feed (supernatants phosphate enriched). The C3 sample is withdrawn from the de-aeration column bottom, and it represents the real plant effluent. The C4 sample represents the recycle flowrate.

For the acknowledge of crystallisation and phosphorous removal processes here some key parameters should be taken into account (Fig.7):

- the nucleation efficiency ($\eta\%$): % removed phosphate
- the precipitate efficiency (L%): % phosphate leaving the FBR with the effluent as small MAP and HAP particles
- the conversion efficiency (X%): $\eta\% + L\%$

The parameters listed above can be calculated as follows:

- Nucleation efficiency: $\eta\% = 100 \frac{(PO_{4\text{tot in}} - PO_{4\text{tot out}})}{PO_{4\text{tot in}}}$;
- Precipitate efficiency (L%): $L\% = 100 \frac{(PO_{4\text{tot out}} - PO_{4\text{sol out}})}{PO_{4\text{tot in}}}$;
- Conversion efficiency (X%): $X\% = \eta\% + L\% = 100 \frac{PO_{4\text{tot in}} - PO_{4\text{sol out}}}{PO_{4\text{tot in}}}$;
- % phosphate crystallized as MAP as to total phosphate removal:

$$\text{PO}_4 - \text{MAP}\% = \frac{(\text{Mg}_{\text{in}} - \text{Mg}_{\text{out}})_{\text{mol}}}{(\text{PO}_{4\text{totin}} - \text{PO}_{4\text{totout}})_{\text{mol}}};$$

- % phosphate crystallized as HAP as to total phosphate removal:

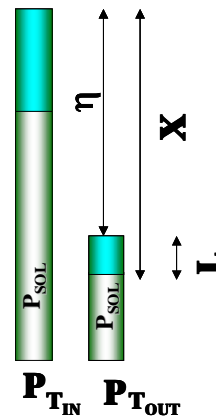
$$\text{PO}_4 - \text{HAP}\% = \frac{(\text{PO}_{4\text{totin}} - \text{PO}_{4\text{totout}})_{\text{mol}} - (\text{Mg}_{\text{in}} - \text{Mg}_{\text{out}})_{\text{mol}}}{(\text{PO}_{4\text{totin}} - \text{PO}_{4\text{totout}})_{\text{mol}}}$$

Figure 7 - Removal efficiency definition

$$\eta \% = \frac{P_{TOT\text{in}} - P_{TOT\text{out}}}{P_{TOT\text{in}}} 100$$

$$L \% = \frac{P_{T\text{out}} - P_{S\text{out}}}{P_{T\text{in}}} 100$$

$$X \% = L \% + \eta \%$$



2.11 Data sheets

All the main parameters are daily recorded and organized in data sheets during the monitoring of the plant to have the complete database of the plant operational conditions as well as the physical-chemical characteristics. Table 6 is an example.

Table 6 - Data sheet example

Day	Q from press	Q inlet	Q ricir	Q air	pH	ORP	T air	T inlet
	m ³ /h	m ³ /h	m ³ /h	Nm ³ /h		mV	°C	°C
01/02/02	4.3	0.1	0.8	11.3	8.90	146.9	10.8	10.7

Generally knowing the feed and effluent characteristics is sufficient; sometimes, though, especially when fines are suspected to escape from the Dortmund, the analysis of the Dortmund sample turns out to be necessary. Table 7 shows the complete data sheet.

Table 7 – Complete data sheet

Stripper Feed

Day	pH	CO ₃	HCO ₃	P _{tot}	P-PO ₄	Ca	Mg	K	N-NH ₄	N-NO ₂	N-NO ₃	SO ₄	TSS	TCOD	SCOD
		mg/l	mg/l	mg/l	mg/l	mg/l	mg/l	mg/l	mg/l	mg/l	mg/l	mg/l	mg/l	mg/l	mg/l

Dortmund

Day	pH	CO ₃	HCO ₃	P _{tot}	P-PO ₄	Ca	Mg	K	N-NH ₄	N-NO ₂	N-NO ₃	SO ₄	TSS	SCOD
		mg/l	mg/l	mg/l	mg/l	mg/l	mg/l	mg/l	mg/l	mg/l	mg/l	mg/l	mg/l	mg/l

FBR outlet

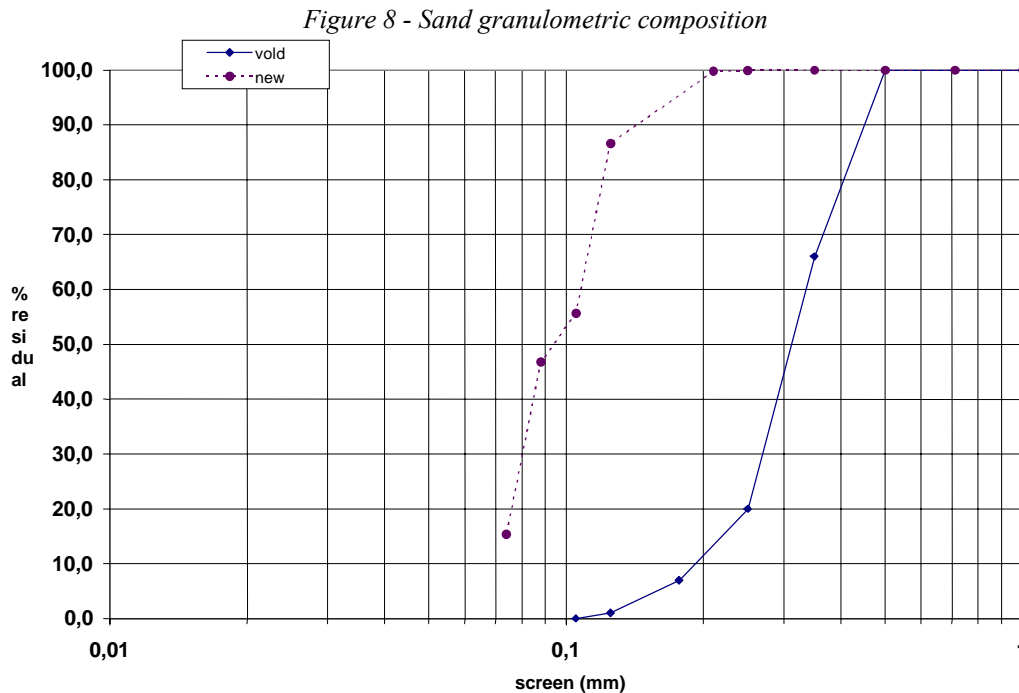
Day	pH	CO ₃	HCO ₃	P _{tot}	P-PO ₄	Ca	Mg	K	N-NH ₄	N-NO ₂	N-NO ₃	SO ₄	TSS	SCOD
		mg/l	mg/l	mg/l	mg/l	mg/l	mg/l	mg/l	mg/l	mg/l	mg/l	mg/l	mg/l	mg/l

3. Results and discussion

3.1 Start up

3.1.1 Sand

The FBR reactor was filled up with 600 kg of silica sand and the material was struvite grooved up. In figure 8 the granulometric composition of two different sands is described, the first one referring to the “old” sand used in the pilot plant and the second one to the “new” sand.



3.1.2 Operational parameters

a) Q_{press}

This parameter represents the flowrate ($< 9 \text{ m}^3/\text{h}$) from the belt press. In the dewatering section it is provided with a stocking tank where the anaerobic supernatant is collected. By the experience it could be observed that using high flowrates ($> 9 \text{ m}^3/\text{h}$), a high solid concentration occurs. For this reason the pumps are set as to prevent the inlet of solid from the dewatering section.

b) Q_{feed}

The FBR feed is kept constant (1 or $1.5 \text{ m}^3/\text{h}$), so as to have a continuous working and a retention time compatible with the process.

c) Q_{recycle}

The recycle flow rate remains constant to promote the fluidised bed and to avoid sand loss through the Dortmund. The proper value was determined considering the settling velocity of a particle that is a function of the fluid properties and of the characteristics of the solid particles. The final settling velocity for a discrete particle is represented by the Stokes' law:

$$v = \frac{g\phi^2(\rho_s - \rho)}{18\mu}$$

where g is gravity acceleration (9.8 m/s^2), μ is the absolute dynamic viscosity of water (kg/m^3), ρ the particle density (kg/m^3), ρ_s the sand density (kg/m^3) and ϕ the spherical particle diameter (m). On the basis of the particles diameter the settling velocity in the FBR reactor, is determined.

To fluidise the bed and to keep the sand in suspension, the velocity of the rising liquid must have opposite direction and equal or higher modulus than the particles falling velocity. The minimum value of the flowrate necessary to keep the bed fluidised can be deduced by the following equation, that defines the surface hydraulic loading rate:

$$C_{is} = \frac{Q}{A}$$

From this equation the percentage of fluidized bed is determined .

In the first column of table 8 the theoretical flowrate value is reported; in the second column the surface hydraulic loading rate is determined on the basis of the daily flowrate considering a reactor diameter of 0.6 m.. In the third column the largest particle diameter that may be fluidized with this Q_r value is reported and in the last column the percentage of really fluidized sand on the total, determined by the granulometric distribution.

Table 8 - Q recycle

Q recycle m ³ /h	C_{is} m/h	d max fluid mm	% fluidized bed
4	14,15	0,066	0% - 15%
6	21,23	0,081	15% - 47%
8	28,31	0,094	47% - 56%
10	35,39	0,105	55.6%
12	42,46	0,115	56% - 87%
14	49,54	0,124	87%
16	56,62	0,133	87% - 99.8%
18	63,69	0,141	87% - 99.8%
20	70,77	0,148	87% - 99.8%
35	123,85	0,196	87% - 99.8%

d) Q_{air}

The air flowrate in the stripping column is necessary to strip CO_2 and to increase pH.

Then the selected flowrate depends on pH and on the inlet flowrate. For this purpose a lot of stripping tests have been carried out.

3.1.3 Hydraulic tests

To test the hydraulics and the electromechanics of the plant a first run was carried out. In the SCP plant, for each volume and flowrate an equivalent HRT exist, according to the “double saturational program model ” (Battistoni *et al.*, 2002).

$$HRT_T = \frac{(V_1 + V_2 + V_3)}{Q_i}$$

$$HRT_{stripp} = \frac{(V_1 + V_2)}{Q_i}$$

$$HRT_{FBR} = \frac{V_3}{Q_{RIC}}$$

$$HRT_{EXP} = \frac{V_{EXP}}{Q_{RIC}} \varepsilon$$

$$n = \frac{HRT_T}{HRT_{FBR}}$$

$$t_c = n \cdot HRT_{EXP} = \alpha \varepsilon \frac{V_{tot}}{Q_i}$$

- HRT_T is the average retention time in the SCP (V_1 is the stripper volume, V_2 the de-aeration column volume, V_3 the total FBR volume including the Dortmund, pipes and the filter);
- HRT_{stripp} is the average retention time in the stripping reactor;
- HRT_{FBR} is the average retention time in the FBR;
- HRT_{exp} is the average retention time in the fluidized bed (the FBR zone in which there is the expanded sand and the empty spaces represent the real available volume = $V_{exp} \cdot \varepsilon$);
- n is the number of liquid recycles done in the FBR reactor, defined as the ratio of the total HRT to FBR HRT;
- t_c is the contact time in the sand, defined as the ratio of HRT_{exp} to the run number in FBR.

3.1.4 Air stripping tests

In order to estimate the influence of the hydraulic loading rate on the de-aeration-stripping system, the same batch tests were carried out with the same inlet flowrate and different air flowrates ($Q_{in} = 1 \text{ m}^3/\text{h}$). These tests demonstrated that the pH value reached 8.5. Moreover the methodology used required a continuous feeding of the stripping column, and then the FBR feeding with the recycle flowrate. Figure 9 shows the results obtained.

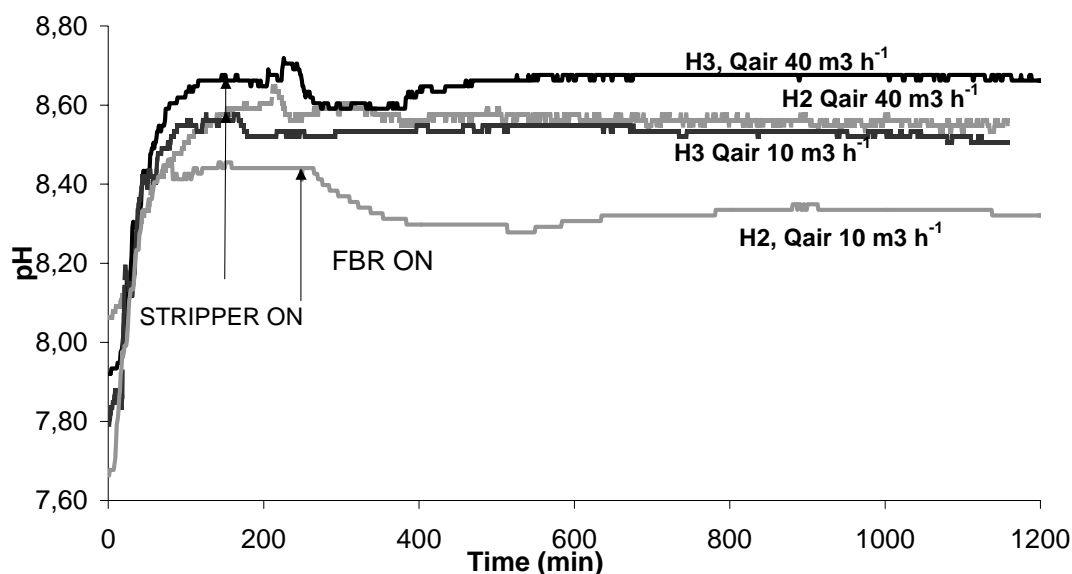
When the FBR was operating the hydraulic retention time changed, becoming HRT_T (from HRT_{strip} to HRT_T , see equations above).

The results demonstrated that to get an operational pH = 8.3 or higher, the highest hydraulic loading rate should be applied (H3) together with the lowest air flowrate ($Q_{air} = 10 \text{ m}^3/\text{h}$). Working with the lowest hydraulic flowrate value (H1 or H2), the air flowrate must be increased ($Q_{air} = 40 \text{ m}^3/\text{h}$).

The highest pH reached was 8.7; this was, however, lower than the one achievable with a typical anaerobic supernatant. This was mainly due to the low alkalinity value in the liquid used ($1000 \text{ mgCaCO}_3/\text{l}$).

The de-aeration column pH-meter is continuously measuring and this facilitates the adjustment of the air flowrate according to the chosen operational parameters.

Figure 9 - pH increase in different operational conditions



During this test scum production was observed when increasing aeration: this made the situation unmanageable in H₃ because of the scum overflow from the reactor. A flowrate value of about 40 m³/h is manageable only if gradually reached. The pH sensor had to be daily cleaned and calibrated.

3.1.5 Phosphorous addition

Since the biological nutrients removal process in wastewater treatment was not fully developed, only a little content of phosphorous was present in the sludge, therefore the P concentration in the surnatants after the anaerobic digestion process was low. In order to better identify the SCP performances P salts were added to the surnatants so to increase the P-PO₄ concentration.

3.1.6 Preliminary tests

a) Natural ageing tests

Natural ageing tests on the anaerobic supernatant taken from the dewatering section and on the supernatant added with the appropriate amount of phosphate were carried out, to understand the phosphate influence on the removal process and on the preferential phosphate conversion.

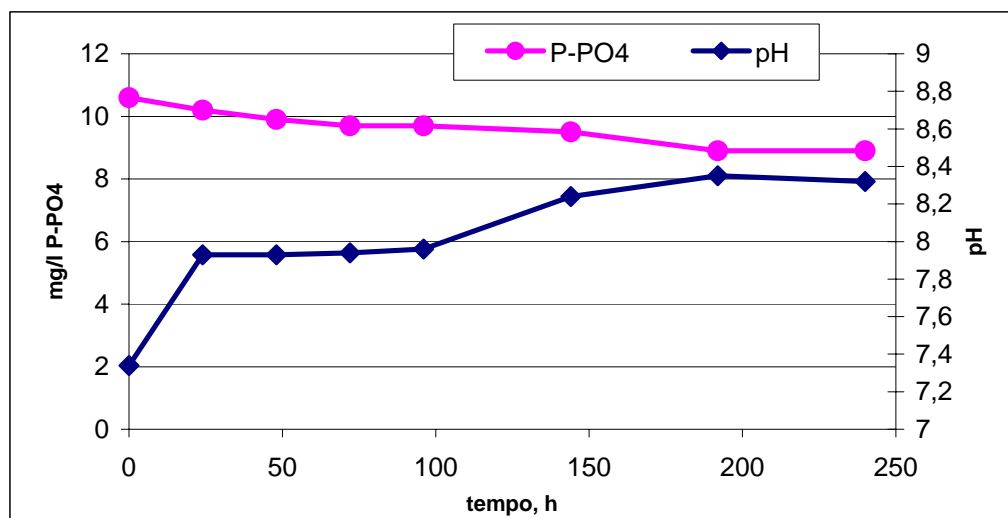
First natural ageing test: the natural supernatant was kept in a thermostatic room (25°C). Daily samples were withdrawn and analysed. Table 8 and figure 10 show the results.

Table 8 - Chemical-physical characteristics of the anaerobic supernatant during the first natural ageing test.

t h	pH	Alk mg/l	P-PO ₄ mg/l	Ca _{sol} mg/l	Mg _{sol} mg/l	K _{sol} mg/l	P _{tot} mg/l	N-NH ₄ mg/l	Ca mmol	Mg mmol	P mmol	Ca/Mg	Ca/PO ₄	Mg/PO ₄
0	7,34	670	10,6				12,02	163,4			0,34			
24	7,93	740	10,2	126,1	38,5	30			3,15	1,58	0,33	1,99	9,55	4,81
48	7,93	905	9,9	90,3	34,4	28			2,25	1,42	0,32	1,59	7,05	4,43
72	7,94	875	9,7								0,31			
96	7,96	870	9,7	120,7	39	27,2			3,01	1,60	0,31	1,88	9,62	5,12
144	8,24	815	9,5								0,31			
192	8,35	720	8,9								0,29			

The main trends were the decrease of phosphate (from 10.6 mg/l to 8.90 mg/l), the increase of pH and the molar losses (0.05 mmols).

Figure 10 - pH and soluble phosphate concentration trends, during the first natural ageing test.



The second ageing test was carried out on the supernatant added with phosphate, reaching a concentration of 48 mgP/l., in order to investigate the behaviour at different phosphate concentrations.

Table 9- Chemical-physical characteristics of the supernatant added with phosphate during the second ageing test.

t h	pH	Alk mg/l	P-PO ₄ mg/l	Ca _{sol} mg/l	Mg _{sol} mg/l	K _{sol} mg/l	P _{tot} mg/l	N-NH ₄ mg/l	Ca mmol	Mg mmol	P mmol	Ca/Mg	Ca/PO ₄	Mg/PO ₄
0	7,34	725	48	112,9	40,2	31,6	48	177,2	2,82	1,65	1,55	1,70	1,82	1,07
24	7,71	985	47,7	83,88	37,3	30,2			2,09	1,53	1,54	1,36	1,36	1,00
48	7,71	950	46	107,5	36,4	31,3			2,68	1,50	1,49	1,79	1,81	1,01
72	7,8	860	43,3	127,4	40,7	30,2			3,18	1,67	1,40	1,90	2,27	1,20
96	7,9	955	41	107,3	37,9	29,9			2,68	1,56	1,32	1,72	2,02	1,18
144	8,1	845	37,9								1,22			
192	8,12	865	32,3								1,04			
240	8,14	855	27,6				28,6				0,89			

The results obtained are in accordance with the results of the first test even though the decrease of phosphate concentration is more evident in this test: in fact phosphate concentration decreased from 48 mg/l to 27.6 mg/l. pH increased from 7.34 to 8.14. Figure 11 shows pH and phosphate concentration behaviour during this test.

The third natural ageing test was carried out on the supernatant enriched with 50 mgP/l adding (NH₄)₂HPO₄ (see table 10). These runs demonstrated that the phosphate initial concentration is an important parameter to promote phosphate precipitation. Figure 12 shows the phosphate decrease (from 51 mgP/l to 33 mgP/l) and the pH increase (from 7.37 to 7.98).

The percentage of phosphate conversion was defined as the ratio between P-PO₄ in solution and P-PO₄ at the beginning; then the conversion during each natural ageing tests was analysed considering also the Ca/Mg, Ca/PO₄ and Mg/PO₄ molar ratios. In fact the evolution of the molar ratios allowed the acknowledge of the phosphate salt formation (struvite or hydroxyapatite).

The highest phosphate removals were obtained when the supernatant was phosphate enriched. The P conversion moved from 8.7% in the natural supernatant to 35-36% in the phosphate added supernatants.

Figure 11 - pH and phosphate concentration trends during the second natural ageing test

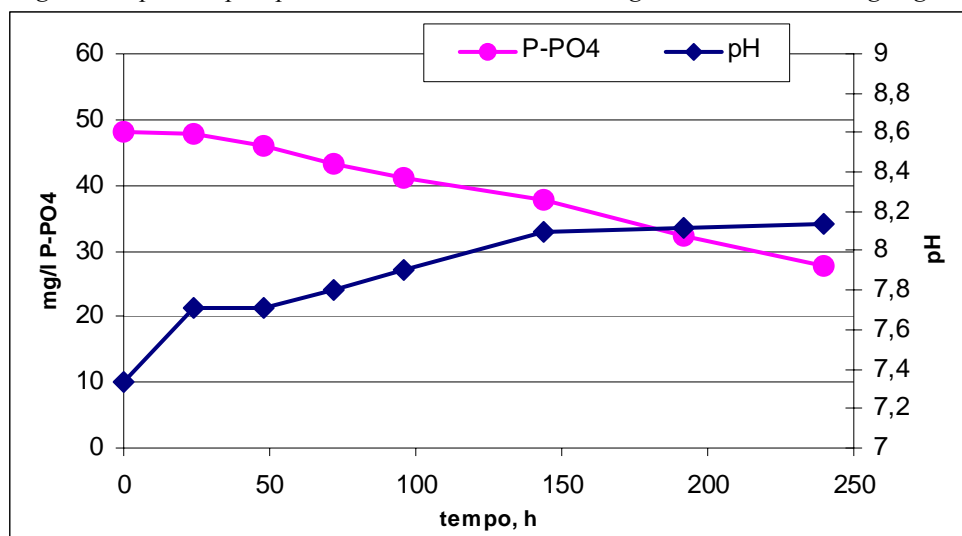
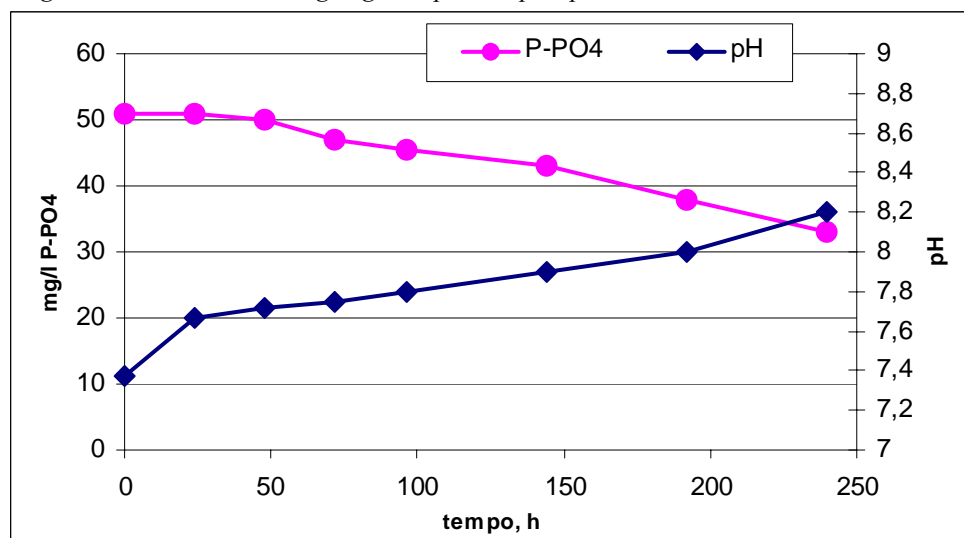


Table 7 - Third natural ageing test, sample phosphate added up to 50 mgP/l: chemical-physical characteristics

t h	pH	Alk mg/l	P-PO ₄ mg/l	Ca _{sol} mg/l	Mg _{sol} mg/l	K _{sol} mg/l	P _{tot} mg/l	N-NH ₄ mg/l	Ca mmol	Mg mmol	P mmol	Ca/Mg	Ca/PO ₄	Mg/PO ₄
0	7,37	785	51	96,09	35,2	25,8	56,7	229,8	2,40	1,45	1,65	1,66	1,46	0,88
24	7,67	1100	51	149,7	49,4	14,8			3,74	2,03	1,65	1,84	2,27	1,23
48	7,72	940	50	123,6	42,1	29,3			3,08	1,73	1,61	1,78	1,91	1,07
72	7,75	905	47	122,1	38,9	29,6			3,05	1,60	1,52	1,90	2,01	1,05
96	7,8	940	45,5	88,85	28,1	30,8			2,22	1,16	1,47	1,92	1,51	0,79
144	7,9	840	43								1,39			
192	8	870	38								1,23			
240	8,2	695	33				37,9				1,07			

Figure 12 - Third natural ageing test: pH and phosphate concentration trends with time.



The Ca and Mg molar ratios strongly influenced the kind of phosphate salt formation; furthermore the tests confirmed the slow evolution of the system towards supersaturation conditions.

b) Supersaturation tests

First supersaturation test. In order to study the MAP or HAP formation it is important to consider the influence of phosphate and magnesium concentration.

First curve: phosphate concentration was increased from 20 mgP/l to 54 mgP/l, adding $(\text{NH}_4)_2\text{HPO}_4$; pH increased by adding alkali until the nucleation pH value was reached. Table 11 shows the results.

Table 8 - First curve- first supersaturation test

P-PO ₄ , mg/L	Initial pH	pH*	mg/L NaOH added
20	7,62	9,07	0,5
22	7,69	8,74	0,4
28,5	7,76	8,43	0,3
42	7,59	8,33	0,16
54	7,58	8,22	0,2

Second curve: phosphate concentration was increased from 20 mgP/l to 52.5 mgP/l adding $(\text{NH}_4)_2\text{HPO}_4$; each sample was also added with 50 mg/l of MgCl_2 . pH was increased adding alkali until the nucleation pH value was reached. Table 12 shows the results.

Table 9 - Second curve – first supersaturation test

P-PO ₄ , mg/L	Initial pH	pH*	mg/L NaOH added
20	7,62	9,07	0,5
23	7,9	8,7	0,45
28,5	7,63	8,52	0,4
43,4	7,5	8,4	0,3
55,2	7,7	8,2	0,2

Third curve: phosphate concentration was increased from 20 mgP/l to 68 mgP/l adding H_3PO_4 ; pH was increased by adding alkali until the nucleation pH value was reached. Table 13 shows the results.

Table 10 - Third curve – first supersaturation test

P-PO ₄ , mg/L	Initial pH	pH*	mg/L NaOH added
20	7,62	9,07	0,5
32,5	7,45	8,5	0,38
39	7,33	8,4	
46,9	7,26	8,35	0,4
68	7,15	8,28	0,45

The trends in figure 13 show that when the phosphate concentration in solution increases, then the pH value necessary for the nucleation decreases. The magnesium salt added (second test) didn't produce a different salt (the curve didn't shift), probably because of the high magnesium concentration in the natural supernatant. The same behaviour was observed in the third test, where H_3PO_4 was added instead of $(\text{NH}_4)_2\text{HPO}_4$.

Second supersaturation test. This second set of test was carried out to investigate the effect of different supernatants on MAP or HAP formation. To perform this tests the real supernatant was added with an appropriate amount of phosphate as $(\text{NH}_4)_2\text{HPO}_4$.

Figure 13 - Supersaturation curves- third set of test

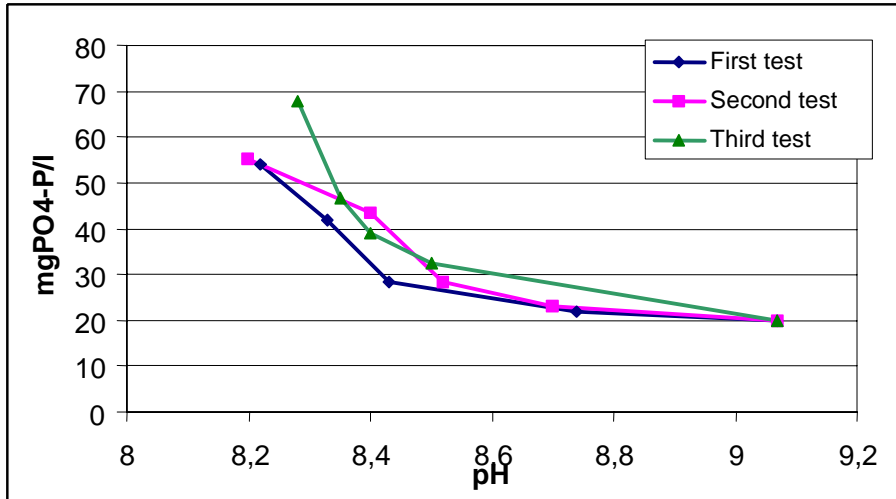


Table 11 - First supersaturation test- second set of tests

pH*	Initial pH	P-PO ₄ , mg/L	N-NH ₃ , mg/L	ml NaOH added
9,46	7,98	10,3	118	0,65
8,57	7,93	14,5	130	0,2
8,2	7,64	24,32	138	0,08
7,98	7,6	38	155	0,075

Table 12 - Second supersaturation test- second set of test

pH*	Initial pH	P-PO ₄ , mg/L	N-NH ₃ , mg/L	ml NaOH added
8,83	7,69	11,4	103,7	0,4
8,4	7,69	15	114	0,3
8	7,68	22,9	137,7	0,1
7,88	7,68	27,7	290	0,08
7,71	7,65	50,4	140	0,06
7,69	7,55	52	322	0,05

Table 13 - Third supersaturation test- second set of tests

pH*	Initial pH	P-PO ₄ , mg/L	N-NH ₃ , mg/L	ml NaOH added
10,4	7,68	8,02	85,18	0,4
9,8	7,64	17,5	90	0,3
8,44	7,7	42,6	103,9	0,1
8,2	7,9	63,7	123	0,1
8,15	7,9	75,1	/	0,1
8,04	7,87	99,7	/	0,08

Table 14 - Fourth supersaturation test - second set of tests

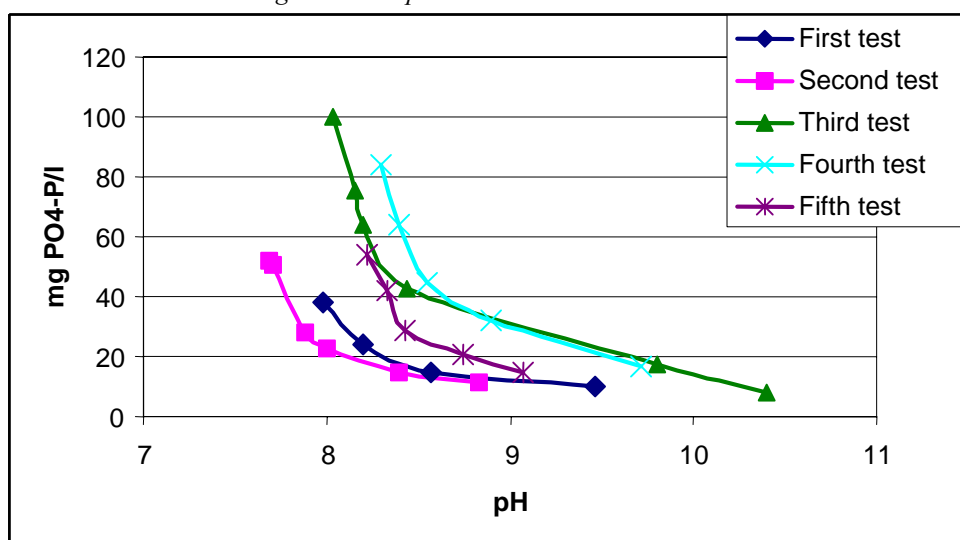
pH*	Initial pH	P-PO ₄ , mg/L	N-NH ₃ , mg/L	ml NaOH added
9,71	7,62	16,8	103,3	0,7
8,9	7,79	31,7	112,2	0,3
8,55	7,84	44,6	131,2	0,2
8,4	7,9	63,8	133,3	0,2
8,3	7,94	84,1	140	0,1

Table 15 - Fifth supersaturation test- second set of tests

pH*	Initial pH	P-PO ₄ , mg/L	N-NH ₃ , mg/L	ml NaOH added
9,07	7,62	15	/	0,5
8,74	7,69	21	/	0,4
8,43	7,76	28,5	/	0,3
8,33	7,59	42	/	0,16
8,22	7,58	54	/	0,2

Figure 14 shows the supersaturation curves obtained.

Figure 14 - Supersaturation curves- second set



The main trends were in accordance with the hypothesis that increasing the phosphate concentration the pH value necessary for nucleation decreases.

It is possible to distinguish two groups of curves: the curves of the first and the second test are translated to a lower pH than the fourth and fifth test curves. This behaviour is due to the prevalent formation of one salt, while the fifth test curves shows the co-formation of MAP and HAP.

Unfortunately during this set of tests the cations were not analysed, so this hypothesis are not confirmed by the ratio between the molar loss of magnesium and calcium; however this behaviour is confirmed by some literature data (Battistoni et al.,1998). On these basis it is believable that struvite is represented by the curves translated to higher pH values, and hydroxyapatite by the curves translated to a lower pH value.

Third set of supersaturation tests. During the third set of tests the supernatant was enriched with H_3PO_4 or $(NH_4)_2HPO_4$ and calcium as $CaCl_2$ to verify the percent of phosphate distribution in MAP and HAP formation. The following tables show the analytical procedures adopted. For each test there are two tables: the first one shows the initial and final (at pH*) phosphate concentrations, the amount of alkali added, the initial and final potassium, magnesium and calcium concentration (mg/l and mmol). The final concentrations, when the supersaturation conditions are obtained, are yellow coloured. In the second table the calculation used to determine HAP, MAP and calcite molar fractions and the percentage of formation of each salt are reported.

Table 16 - First supersaturation test- concentrations

P-PO ₄	P-PO ₄	pH*	NaOH added	N-NH ₄	K	Mg	Ca	P	Mg	Ca/PO ₄	Mg/PO ₄	Ca
mg/l	mg/l		ml/100ml	mg/l	mg/l	mg/l	mg/l	mmol	mmol			mmol
19		7,5		131,6	43,6	46,1	119,8	0,61	1,90	4,88	3,09	2,99
	2,83	9,62	1,45	114,9	43,0	40,8	56,2	0,09	1,68	15,37	18,38	1,40
22				131,2	43,2	44,8	120,8	0,71	1,84	4,25	2,60	3,01
	4,6	8,91	0,6	123,3	42,7	41,2	65,2	0,15	1,69	10,96	11,42	1,63
34				127,8	43,3	39,5	93,1	1,10	1,63	2,12	1,48	2,32
	11,64	8,36	0,5	126,8	43,0	42,4	74,1	0,38	1,74	4,92	4,64	1,85
52				131,1	43,8	45,3	88,7	1,68	1,86	1,32	1,11	2,21
	22,41	8,22	0,45	126,6	42,6	41,2	67,7	0,72	1,70	2,34	2,34	1,69
59,2				130,6	44,4	43,2	88,5	1,91	1,78	1,16	0,93	2,21
	20,12	8,2	0,45	126,4	43,7	41,6	64,2	0,65	1,71			1,60

Table 17 - First supersaturation test- calculations

P as MAP %	P as HAP %	MAP mmol	HAP mmol	Calcite mmol	X MAP %	X HAP %	X CALCITE %
41,88	58,12	0,22	0,10	1,08	15,6	7,2	77,2
26,68	73,32	0,15	0,14	0,70	15,2	13,9	71,0
-16,20	116,20	-0,12	0,28	-0,92	15,4	-36,8	121,4
17,54	82,46	0,17	0,26	0,00	39,0	61,0	0,0
5,29	94,71	0,07	0,40	0,00	14,3	85,7	0,0

The first supersaturation curve (Tab. 19-20) was carried out on the supernatant added with H₃PO₄. With the increasing phosphate concentration, the hydroxyapatite formation increased instead of calcite.

During the second test the supernatant was enriched with H₃PO₄ and CaCl₂ to increase the calcium concentration to about 150mg/l. Table 21-22 shows the results.

Table 18 - Second supersaturation test- concentrations

P-PO ₄ mg/l	pH*	NaOH added ml/100ml	N-NH ₄ mg/l	K mg/l	Mg mg/l	Ca mg/l	P mmol	Mg mmol	Ca mmol	Ca/PO ₄	Mg/PO ₄	
19												
	8,12	0,25										
22			131,3	42,1	43,9	257,2	0,71	1,81	6,42	9,04	2,55	
	7	7,91	0,15	129,2	42,9	44,0	215,9	0,23	1,81	5,39	23,86	8,02
34			131,5	42,4	43,5	212,2	1,10	1,87	5,30	4,83	1,71	
	9,04	7,54	0,1	119,1	43,8	45,4	214,0	0,29	1,87	5,34	18,31	6,41
52			130,1	42,4	44,4	257,0	1,68	1,82	6,41	3,82	1,09	
	10,71	7,35	0,05	129,9	42,3	41,9	191,9	0,35	1,72	4,79	13,86	4,99
59,2			133,8	43,7	45,5	262,0	1,91	1,87	6,54	3,42	0,98	
	11,1	7,24	0,05	131,2	44,4	44,9	239,7	0,36	1,85	5,98	16,70	5,16

Table 19 - Second supersaturation test- calculations

P as MAP %	P as HAP %	MAP mmol	HAP mmol	Calcite mmol	X MAP %	X HAP %	X CALCITE %
0,00	100,00	0,00	0,16	0,22	0,0	42,0	58,0
0,10	99,90	0,00	0,27	0,00	0,3	99,7	0,0
7,54	92,46	0,10	0,41	0,00	19,6	80,4	0,0
1,62	98,38	0,03	0,51	0,00	4,7	95,3	0,0

Table 20 - Third supersaturation test- concentrations

P-PO ₄ mg/l	pH*	NaOH added ml in 100ml	N-NH ₄ mg/l	K mg/l	Mg mg/l	Ca mg/l	P mmol	Mg mmol	Ca mmol	Ca/PO ₄	Mg/PO ₄	
19			131,64	43,62	46,09	119,77	0,61	1,90	2,99	4,88	3,09	
	2,83	9,62	1,45	114,87	43,02	40,78	56,23	0,00	1,68	1,40		
26,6			136,57	42,71	44,51	115,87	0,86	1,83	2,89	3,37	2,13	
	6,51	8,63	0,45	129,70	42,64	41,47	66,51	0,00	1,71	1,66		
39,2			142,86	42,48	44,64	117,88	1,26	1,84	2,94	2,33	1,45	
	10,24	8,37	0,30	141,04	45,27	41,10	62,19	0,33	1,69	1,55	4,70	5,12
54,6			157,93	43,13	43,88	89,07	1,76	1,81	2,22	1,26	1,03	
	19,60	8,28	0,12	154,51	41,77	37,64	54,73	0,63	1,55	1,37	2,16	2,45
79			165,12	43,16	44,5	117,74	2,55	1,83	2,94	1,15	0,72	
	40,64	7,90	0,10	163,35	42,69	43,23	89,54	1,31	1,78	2,23	1,70	1,36

Phosphate precipitated as HAP instead of MAP (HAP formation 90% higher), moreover when the pH value increased the calcite formation was favoured (58%).

The third test was carried out adding $(\text{NH}_4)_2\text{HPO}_4$. The results are in tables 23-24. Phosphate was removed mainly as hydroxyapatite instead of struvite, and the percentage of calcite formation was smaller than 16%, while it was absent at low pH value, when phosphate concentration increased.

Table 21 - Third supersaturation test-calculations

P as MAP%	P as HAP%	MAP	HAP	Calcite	X MAP	X HAP	X CALCITE
%	%	mmol	mmol	mmol	%	%	%
14,58	85,42	0,13	0,24	0,01	33,0	64,4	2,6
15,59	84,41	0,15	0,26	0,08	30,1	54,3	15,6
22,74	77,26	0,26	0,29	0,00	46,9	53,1	0,0
4,22	95,78	0,05	0,40	0,00	11,7	88,3	0,0

Table 22 - Fourth supersaturation test- concentrations

P-PO ₄	pH*	NaOH added	N-NH ₄	K	Mg	Ca	P	Mg	Ca	Ca/PO ₄	Mg/PO ₄
mg/l	mg/l	ml in 100ml	mg/l	mg/l	mg/l	mg/l	mmol	mmol	mmol		
19	8,12	0,25									
26,6			135,13	43,43	46,28	268,96	0,86	1,90	6,71	7,82	2,22
	5,70	7,71	0,15	133,35	42,15	43,05	202,51	0,18	1,77	5,05	27,48
39,2				143,54	43,15	44,57	242,83	1,26	1,83	6,06	4,79
	10,24	7,49	0,05	142,53	43,05	43,63	204,26	0,33	1,80	5,10	15,43

The fourth supersaturation test was carried out adding calcium as CaCl_2 and $(\text{NH}_4)_2\text{HPO}_4$. In tables 25-26 the results are shown.

Table 23 - Fourth supersaturation test- calculations

P as MAP%	P as HAP%	MAP	HAP	Calcite	X MAP	X HAP	X CALCITE
%	%	mmol	mmol	mmol	%	%	%
19,71	80,29	0,13	0,18	0,76	12,4	16,9	70,7
4,14	95,86	0,04	0,30	0,00	11,5	88,5	0,0

Calcite formation was not observed at low pH values (7.5) while, when the pH value was about 7.7, calcite prevailed. However the removal of phosphate mainly as HAP (80-95%) was observed.

During the fifth test $(\text{NH}_4)_2\text{HPO}_4$ and calcium (100 mg/l) were added. Tables 27-28 show the results.

Table 24 - Fifth supersaturation test- concentrations

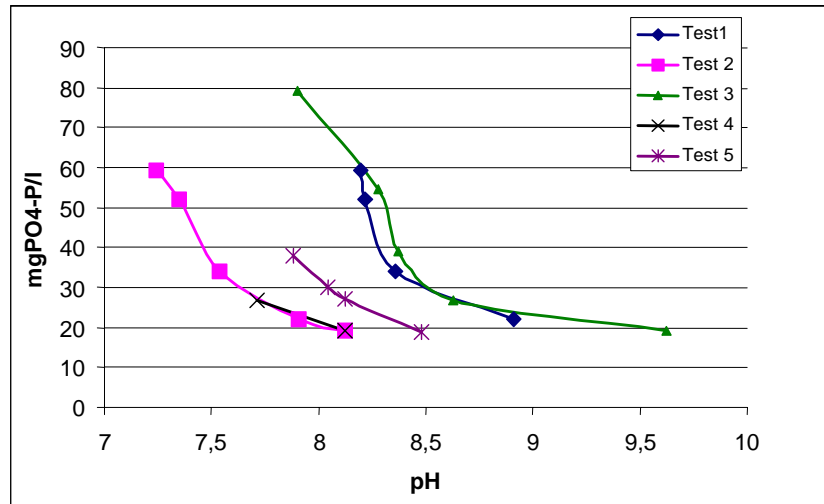
P-PO ₄	pH*	NaOH added	N-NH ₄	K	Mg	Ca	P	Mg	Ca	Ca/PO ₄	Mg/PO ₄
mg/l	mg/l	ml in 100ml	mg/l	mg/l	mg/l	mg/l	mmol	mmol	mmol		
18,8			130,27	43,85	46,99	231,01	0,61	1,93	5,76	9,50	3,19
	3,77	8,48	8,3	125,75	42,82	43,87	168,39	0,12	1,80	4,20	34,55
27				139,71	43,88	46,45	211,21	0,87	1,94	5,27	6,05
	14,39	8,12	8,2	136,88	44,58	47,25	185,32	0,46	1,94	4,62	9,96
30				140,98	43,18	45,44	206,71	0,97	1,87	5,16	5,33
	15,94	8,04	0,08	141,56	43,84	45,26	176,37	0,51	1,86	4,40	8,56
38				154,6	43,71	45,92	185	1,23	1,89	4,62	3,77
	21,93	7,88	0,02	151,85	42,9	44,32	147,38	0,71	1,82	3,68	5,20

Table 25 - Fifth supersaturation test- calculations

P as MAP%	P as HAP%	MAP	HAP	Calcite	X MAP	X HAP	X CALCITE
%	%	mmol	mmol	mmol	%	%	%
26,48	73,52	0,13	0,12	0,97	10,6	9,8	79,7
0,00	100,00	0,00	0,14	0,00	0,0	100,0	0,0
1,63	98,37	0,01	0,15	0,01	4,4	87,7	7,9
12,70	87,30	0,07	0,15	0,18	16,4	37,6	46,0

This test showed a removal of phosphate as HAP. The percentage of MAP, HAP and calcite conversions was apparently anomalous because of their variability during the test. The trends of the five supersaturation curves are shown in figure 15.

Figure 15 - Supersaturation curves – thirst set



The figure shows two supersaturation curves (1 and 3) in the high pH area, and two curves (2 and 4) in the lower pH value. The fifth curve is located between the two groups. The first group is characterised with a higher percentage of MAP conversion (peak of 39%-47%). Test 2 4 and 5 are made adding also CaCl₂: the availability of Ca, also for low pH value, determines HAP formation rather than MAP formation. In tests number 1 and 3 Ca is used for calcite formation which is not hindered by the low alkalinity value: P can precipitate as HAP rather than MAP. Sovrasaturation curves in which HAP formation is preponderant are located in the left side while the curve located in the right side indicate struvite precipitation (*Battistoni et al., 1998*)

c) Plant

Once the preliminary tests and the start up phase of the plant were finished, in March 2001 the crystallization test began.

The first set of tests was carried out from March 2001 to May 2001. During these tests a high loss of phosphate as fine particles was observed, and consequently a lower phosphate removal performance; therefore the Dortmund was modified. To permit this, the plant operation was stopped from May to June 2001. From July to September the plant re-started working continuously.

Another stop was necessary in October because of the inlet pump breakage; afterwards, as a consequence of the outer low temperatures, the inlet froze.

In February the plant was restarted for crystallization new tests until May 2002.

The analyses done during this period show a lightening of the bed because of the presence of solid high concentration in the treated liquid. To restart the tests it was necessary to change the sand bed with a clean one. From June 2001 the plant was able to work continuously except in August when the staff was in summer break. Table 26 shows the periods in which the plant was in operation.

Table 26 - Periods of plant operation

Period		
I period	March 2001-May 2001	
stop	May2001 – June 2001	Dortmund modification
II period	July 2001-September 2001	
stop	October 2001-January 2002	Pumps breakage – water freezing
III period	February 2002-March 2002	
stop	April 2002 - May 2002	Cleaning and sand bed replacement
IV period	June 2002-September 2002	

d) Crystallization tests

The data-logger is able to record the signals registered by the transmitters. In the first months the data-logger was broken, so the main parameters as pH and the flowrates were registered manually. Table 30 shows the operational parameters of SCP during the period. Table 31 and 32 show the concentration of the inlet and outlet samples. The analyses of cations were done in the laboratory of the University of Ancona.

Table 27 - Average parameters

period		Q _{belt press} m ³ /h	Q _{inlet} m ³ /h	Q _{recycle} m ³ /h	Q _{air} Nm ³ /h	pH	ORP mV	T _{air} °C	T _{stripper} °C
july-01	average	1,4	1,4	6,2	35,4	8,1	-136,7	29,2	27,6
	min	0,1	1,4	6,1	33,4	8,0	-274,3	28,4	27,2
	max	3,0	1,4	6,2	38,5	8,2	-2,3	30,9	28,0
	s.d	1,0	0,0	0,1	1,8	0,1	98,3	0,9	0,3
aug-01	average	1,4	1,3	6,1	49,8	8,2	-412,8	28,4	28,2
	min	0,1	0,4	4,4	33,5	7,3	-470,1	26,3	25,7
	max	3,0	1,5	6,3	68,2	8,9	-135,3	29,9	29,8
	s.d.	0,6	0,3	0,3	7,7	0,5	88,7	1,1	1,1
sept-01	average	1,3	1,0	5,4	60,9	8,8	24,0	25,8	25,8
	min	0,1	0,5	0,6	21,6	8,4	21,6	24,0	24,0
	max	3,2	1,2	6,3	117,7	9,0	26,5	27,0	27,0
	s.d.	0,7	0,2	1,9	23,5	0,1	1,4	1,0	1,0
feb-02	average	2,2	0,7	6,1	4,3	9,0	114,3	12,6	16,3
	min	0,2	0,2	5,8	0,0	8,7	12,5	10,6	12,7
	max	4,5	1,2	6,6	15,2	9,3	178,0	15,2	19,8
	s.d.	1,5	0,3	0,2	6,0	0,2	64,5	1,2	2,1
march -02	average	1,4	1,1	4,9	0,5	8,9	-1,1	15,8	19,3
	min	0,2	0,5	4,3	0,0	8,6	-165,0	14,7	17,5
	max	3,1	1,3	6,0	1,1	9,3	133,0	16,8	20,5
	s.d.	0,8	0,2	0,8	0,3	0,2	122,8	0,7	1,0
june-02	average	0,6	0,7	3,9	5,8	9,0		28,8	28,1
	min	0,1	0,0	0,7	1,0	8,5		25,6	22,6
	max	2,8	1,4	6,2	14,7	9,2		35,0	35,6
	s.d.	1,0	0,5	2,2	5,1	0,3		2,7	3,7
july-02	average	0,1	1,2	4,5	27,1	8,8		27,9	27,4
	min	0,0	0,0	0,5	23,1	8,4		25,9	24,7
	max	1,1	2,8	5,3	29,5	9,1		29,2	29,3
	s.d.	0,2	0,7	1,1	1,8	0,2		1,1	1,2

Table 28 - Inlet concentration

period	pH	P _{tot}	P-PO ₄	N-NH ₄	K	Mg	Ca	Alk-M	P	Mg	Ca
		mg/l	mg/l	mg/l	mg/l	mg/l	mg/l	mg/l	mmol	mmol	mmol
31/03-15/04 2002	7,6	23,7	18	31,5	30,7	39,7	125,7	962	0,58	1,63	3,14
15/04-14/05-2002	7,6	33,8	23,3						0,75		
july-02	7,7	17,1	15,6						0,5		
ago-02	7,5	15,8	15						0,48		
sept-01	7,8	14,3	12,6								
feb-02	8	72,8	47,9						1,54		
mar -02	7,9	34,3	21,6						0,7		
June-02	7,9	29,8	30,4	286	47,3	33	117,5		0,98	1,36	2,93
july-02	7,9	64,9	51,6	250,7	63,3	34,4	67		1,67	1,41	1,67

The feed had an alkaline pH value; the phosphate concentration was varying since it depended on the addition of (NH₄)₂HPO₄. The results obtained in terms of phosphate conversion were different from month to month. With the exception of these three events, the conversion ranged from 65 to 70%. The nucleation efficiency obtained was not as expected since there was a high percentage of phosphate loss as fine particles.

Table 29 - Outlet concentration

period	pH	P _{tot}	P-PO ₄	N-NH ₄	K	Mg	Ca	Alk-M	P	Mg	Ca
		mg/l	mg/l	mg/l	mg/l	mg/l	mg/l	mg/l	mmol	mmol	mmol
31/03-15/04 2002	8,2	10,98	9,28	23,47	31,9	36,5	103,6	827,3	0,3	1,5	2,59
15/04-14/05-2002	8,5	14,73	12,11						0,39		
july-02	8,4	12,15	8,72						0,28		
aug-02	8,4	11,98	6,86						0,22		
sept-01	8,5	11	8,1						0,26		
febb 2002 C4	8,3	30,7	18,01						0,58		
febb 2002 final	8,5	44,77	24,07						0,78		
march 2002 C4	8,3	25,53	9,74						0,31		
march 2002 final	8,4	26,8	12,05						0,39		
june-02	8,4	44,87	16,65			27,7	81,75		0,54	1,14	2,04
july-02	8,3	35,24	22,6	204,8	54,8	33,6	45,64		0,73	1,38	1,14

*the sample was taken from C4 instead of C3

period	X%=	η%=	L%=
31/03-15/04 2002	60,8	53,6	7,2
15/04-14/05-2002	64,1	56,4	7,8
july-02	49,1	29,0	20,1
aug-02	56,6	24,3	32,4
sept-01	43,2	23,4	19,8
feb2002 C4	75,3	57,9	17,4
feb 2002 final	67,0	38,5	28,4
march 2002 C4	71,6	25,6	46,1
march 2002 final	64,9	21,9	43,0
June-02	44,2	-50,5	94,6
July-02	65,2	45,7	19,5

The third time the parameters were elaborated as the average of the month; then new test will be carried out and the daily parameters will be elaborated in detail, identifying sub-periods characterized by homogeneous parameters. In this way the calculated efficiency and the comparison of it with an hypothetical mathematical model will be really worthy.

Within the inlet and outlet analyses, the bed analyses were done to determinate the following parameters:

- the bed fluidisation (V'10 test);
- the growth of salt grains (granulometric analysis and bed porosity);
- the sand grains composition (chemical analysis).

a) V'10 test

The V'10 tests on the dewatered samples taken from the four different sampling ports of the FBR reactor were performed. Examining the results we can make the following deductions

:

- the recycle flowrate determines the fluidity of the bed, with the exception of the months of April and May during which the V'10 top value was very different from the bottom one.
- Month after month the bed lightened, in fact the same volume of sand, dewatered in March and April, had a lower weight than the silica dewatered in the previous month; this happened because the silica enriched with the solids present in the anaerobic supernatant coming from the belt press. For this reason the dirty sand had to be replaced with new sand. The replacement was done in June 2002 and, for this reason, the sample of July 2002 had a higher weight.
- The bed concentration is used to determinate the volume of sand present in the reactor before the sand replacement; in particular, assuming a bed volume of 0.9 m³ and a maximum sand concentration of 200 g/l, the total sand in the reactor might be 180 kg, lower than the sand really present in the FBR reactor. The hypothesis are:
 - a large amount of silica was lost during the test;
 - in the FBR bottom there was a thick layer of compact sand. This hypothesis will be confirmed during the bed cleaning.

Table 30 - V'10 test

	H1(bottom)		H2		H3		H4(top)	
	V' 10 (ml/l)	gr/l	V' 10 (ml/l)	gr/l	V' 10 (ml/l)	gr/l	V' 10 (ml/l)	gr/l
oct-01	260	157,4	260	158,9	270	160,7	275	169,7
feb-02	352		358		365		365	
feb-02	420		400		400		410	
mar-02	345	167,5	345	167,5	355	174,1	365	179,9
mar-02	340		340		350		355	
mar-02	550		490		290		240	
apr-02	415	180	280	113	280	114,5	290	115,2
may-02	380		340		340		190	
			New bed					
june-02	280		280		280		280	
july-02	500	362	500	357,6	500	360	490	357

b) Test of the exhausted bed

One further test to estimate the grains growth is the granulometric analysis of the dewatered sand sample taken from the FBR reactor. The samples were withdrawn from the four different sampling ports of the FBR, as described in “materials and methods”. Fig.16 and 17 show the results. There was an increase in grains diameter, in fact the granulometric curves are shifted on the right part of the diagram. Figure 16 shows the results of the first bed and figure 17 of the second one.

c) Bed porosity

Bed porosity is the third analysis used to determine the bed volume increase caused by phosphate crystallization (hydroxyapatite/ struvite), as explained in the “materials and methods” section.

The calculation of porosity is made in the same sample where the granulometric distribution was determined. The result of the porosity test is in accordance with the result of the granulometric test since porosity decrease with time.

Table 31 - Bed porosity

First bed	
virgin sand	0,74
September	0,72
October	0,67
February	0,67
March	0,67
Second bed	
Virgin sand	0,80
July 2001	0,78

Figure 16 - Granulometric analyses of the first bed

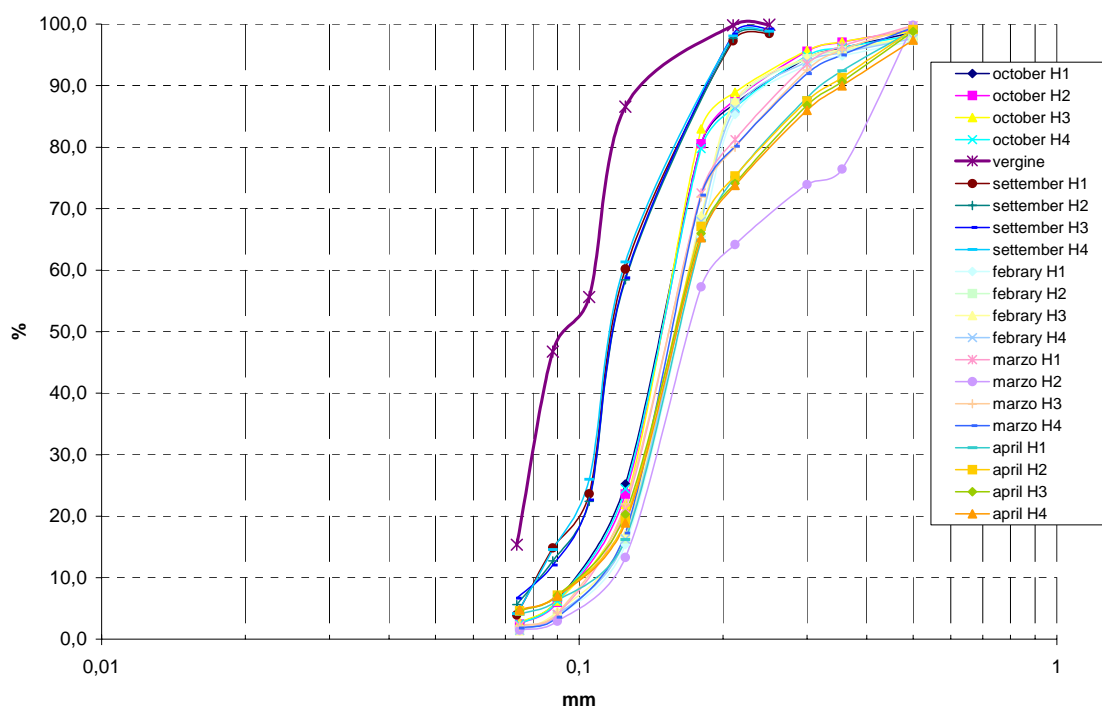
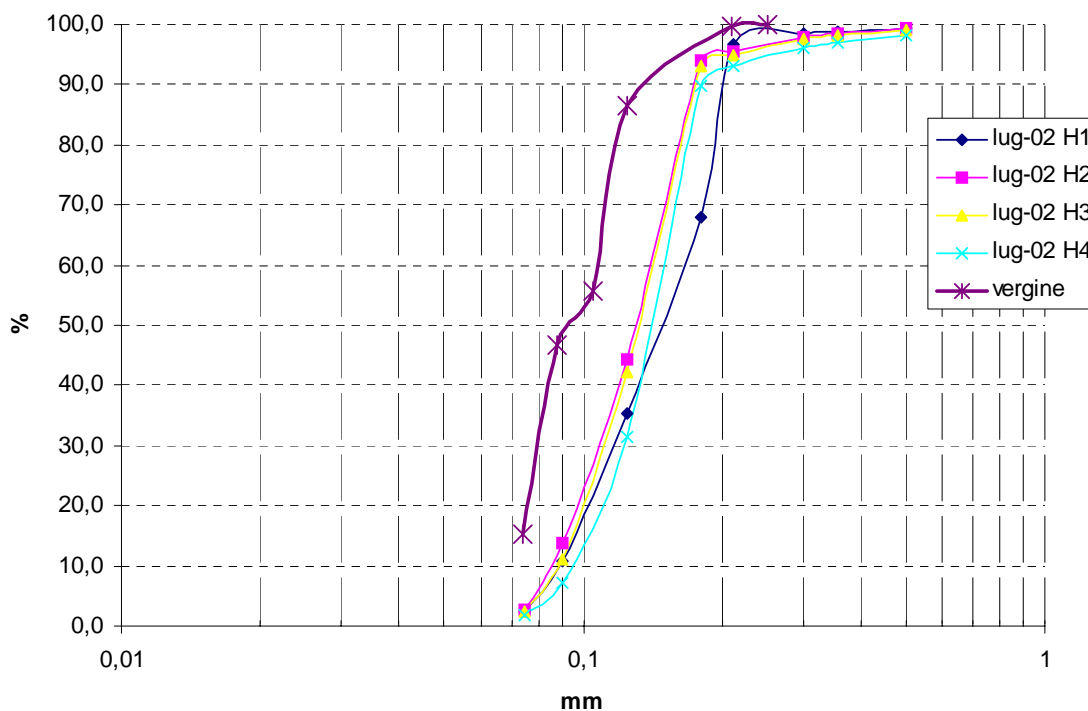


Figure 17 - Granulometric analyses of the second bed



d) Chemical analysis of the sand

Table 32 shows the results obtained by the chemical analysis of the quartz sand. The weight of sand increased: at the end of February (13/02/02), the weight of virgin sand increased more than 30%, in March the value reached 46%. In July the value decreased at 21%, in fact in June the bed was filled up with new quartz sand.

Table 32 - Analyses of silica sand

	Grains composition					
	Weight increase %	silica %	MAP %	HAP %	Calcite %	C + al %
13/02/2002	29,80%	69,73%	3,62%	15,13%	3,53%	7,99%
04/03/2002	36,10%	63,91%	6,46%	19,22%	3,41%	7,01%
26/03/2002	39,60%	56,18%	5,22%	19,91%	5,92%	12,77%
25/05/2002	45,70%	52,78%	4,04%	24,74%	0,00%	18,44%
23/07/2002	20,70%	78,80%	2,47%	11,66%	0,24%	6,83%

The results also evidenced that struvite and hydroxyapatite concentration increased until July. HAP formation prevailed over MAP as a consequence of the operational conditions.

From February to March the percentage of phosphate as MAP increased while it decreased in May. Table 32 show the weight of silica, struvite, hydroxyapatite and calcite in the sand grain. The largest parts are silica, then hydroxyapatite (11 - 25%), and a small percentage of calcite(0.2 - 0.9%) and struvite (2 - 6%).

An important parameter is the presence of organic matter on the silica grains (7 - 18%); the source of organic matter are the solid particles in the anaerobic supernatant. The presence of this “film” delay the growth of phosphate crystals around the grain, therefore it is necessary to provide a hindrance to intercept the solids in the feed. Alternatively, the lowest flowrate from dewatering to SCP must be applied: looking at the data registered during the period it is possible to understand how difficult keeping the lowest and constant value of flowrate is.

e) Dortmund replacement

During the first period of experimentation (March -May 2001), a high loss of fine particles was observed. Taking a look at phosphate conversion (i.e. $\eta\%$, X%, L%) phosphate precipitation high values are evident because of the loss of fine particles through the Dortmund. Moreover, by the analyses of silica in the Dortmund, this hypothesis is confirmed. In fact the FBR was filled with sand with a diameter smaller than the diameter of the sand used in the batch test done to project Treviso plant. To prevent the loss of fine particles the Dortmund should be enlarged to create a quiet zone and to detain particles with smaller diameters. Table 33 shows the characteristics of the two Dortmunds.

Table 33 - Dortmund characteristics

Actual conditions					
Φ_{end}	1,2	m	A_{end}	1,13	m ²
$\Phi_{spillway}$	1,14	m	$A_{spillway}$	1,02	m ²
Φ_{in}	0,6	m	A_{in}	0,28	m ²
Modified conditions					
Φ_{mod}	1,88	m	$A_{spillway\ mod}$	2,77	m ²

Now the larger section has a diameter of 1.88 m and the value of the lost sand is very different. The new section, using the same recycle flowrate, can detain particles with smaller diameters: the percent of sand loss is lower than in the previous conditions. This means that the lost sand percentage is lower and it is constituted by grains with a diameter which is smaller than the size effectively detained. (Tab.34). To know the new efficiency of detained fines, we must evaluate the efficiencies after the Dortmund replacement and mainly the value of L%.

Figure 18 - Dortmund replacement

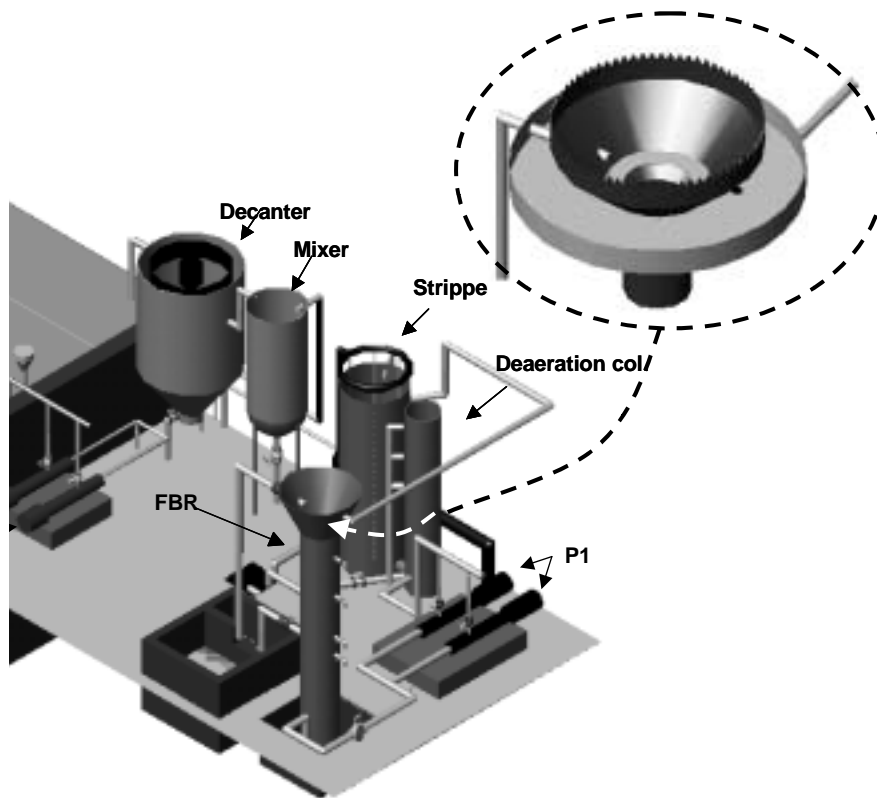


Table 34 – Sand loss with the old Dortmund

Q_{recycle} m ³ /h	Actual $\Phi = 1.14\text{m}$	Modified $\Phi = 1.88\text{m}$
	loss, new SiO ₂ %	loss, new SiO ₂ %
4	10	0 – 15
6	0 – 15	0 – 15
8	0 – 15	0 – 15
10	0 – 15	0 – 15
12	13	0 – 15
14	14	0 – 15
16	15	0 – 15
18	25	0 – 15
20	33	0 – 15
35	55,6	0 – 15
45	86,6	0 – 15

f) The sand bed replacement

The bed replacement became necessary because of the presence of solids in the inlet. The phenomenon was deduced by the results of V'10 tests, and by the progressive bed lightening. Moreover the tests on the grains showed a progressive increase of the organic matter concentration in the sand. On May the 12th the FBR was cleaned up: the silica amount in the reactor was 330 kg plus 150 kg in the Dortmund. About 100 – 150 kg were lost during the experimental period. In the clean reactor a new gravel filter was made with 40 cm of gravel (80mm average diameter) and 40 cm of gravel with an average diameter of 5 – 6 mm. The reactor was filled up with 475 kg of silica (dry silica weight).

On June the 16th the plant was started up with an inlet flowrate of 1 m³/h and a recycle flowrate of 4 m³/h. To test the efficiency of the recycle flowrate, in June a V'10 test was carried out; the results show values homogeneity in the whole FBR.

4. Conclusions and future tasks

The experimental work of these months outlines the easiness of falling into problems that require some project solutions (as the Dortmund replacement), or maintenance solutions (as when the inlet pump was broken) or the necessity to change the sand in the FBR.

Actually the plant is working in good conditions to reach out for the expected results according to the model. To prevent the incoming of organic compounds with the solids coming from the dewatering station, it is necessary to design a specific tank that is able to retain foams rich of volatile solids.

In the future the crystallization tests, in accordance with the adopted methodology, will be performed using different P inlet concentrations. Some test will be done with very high P added to supernatants. Moreover the efficiencies will be calculated, the fluidized bed will be verified, the silica bed will be analyzed (chemical analyses and granulometric tests). New analysis will be made on the sand with the scanning electronic microscopy which will show the real composition of the deposited salts.

Furthermore a study of the mathematical model previously deduced by some tests carried out on laboratory scale will be done; the results obtained will be compared with the expectation of mathematical model.

4.1 The mathematical model

Previous experiments proved that the nucleation efficiency is strongly related to the operative pH, both for experiments carried out on laboratory scale (Battistoni et al., 1998a) and for experiments on a half scale (Battistoni et al., 2001a) but a saturational model is not sufficiently adequate to describe the dependence of nucleation efficiency on process parameters, since a strong dependence of η not only on pH, but also on contact time (t_c) does exist (Battistoni et al., 2001a). Therefore a double saturational model, taking into account for both pH and t_c , was devised, which exhibited an excellent agreement with experimental results. The model is expressed by the following equation (Battistoni et al., 2001b),:

$$\eta\% = 100 \frac{(pH-7.322)}{(pH-7.322)+0.501} \cdot \frac{t_c}{t_c+0.0170}$$

while, as for all the experimental results carried out on the half scale pilot plant (Battistoni et al., 2001a; Battistoni et al., 2001b), the model is represented by the following equation:

$$\eta\% = 100 \frac{(pH-7.329)}{(pH-7.329)+0.440} \cdot \frac{t_c}{t_c+0.0189}$$

A general model, which describes all the experiments carried out on FBR (Battistoni et al., 1998a; Battistoni et al., 2001a + Battistoni et al., 2001b), is the following:

$$\eta\% = 100 \frac{(pH-7.325)}{(pH-7.325)+0.371} \cdot \frac{t_c}{t_c+0.0196}$$

The values of R2 and of S.E. for the above equations are reported in Tab.35.

The introduction of the double saturational model in a pH range which can be easily achieved (from 8.1 to 9.1), allows to fix the most suitable contact time to reach in order to get a prefixed

crystallization efficiency. The conversion (X) and the nucleation (η) must be considered as concomitant phenomena, thus phosphorus removal cannot be optimised considering only the nucleation process on the basis of double saturational model; in fact if the conversion is sensibly higher than the nucleation efficiency, a significant loss of fines is obtained.

Table 35 - R2 and S.E. values

	R ²	S.E.	n*
Battistoni, et al.,2002	0.99	2.3	12
Battistoni, et al.,2002 +Battistoni et al., 2001	0.99	3.3	27
Battistoni, et al.,2002 +	0.99	4.9	44
Battistoni et al., 2000 + Battistoni et al., 2001			

As for the precipitation efficiency (L) it is given by the difference between X and η . The precipitation process is obviously undesired, since it enhances particulate phosphorus escapes with fines and a complex plant is necessary, because a filtration step is needed, thus decreasing the value of η . The behaviour of X as a function of pH can be described by using a saturational model (Battistoni et al., 2001b):

$$X\% = 100 \frac{(\text{pH} - 7.21)}{(\text{pH} - 7.21) + 0.38}$$

for which $R^2=0.99$ and $n= 44$.

5. References

- Battistoni P., De Angelis A., Prisciandaro, M., Boccadoro R., Bolzonella D., (2002). P removal from anaerobic supernatants by struvite crystallization: long term validation and process modelling. *Wat. Res.*, **36** (8), 1927-1938.
- Battistoni P., Fava G., Pavan P., Mata-Alvarez J., (1996). Phosphate removal by crystallization. Anaerobic liquors treated in a fluidized bed reactor. Proceedings of “*Water Quality International 96*”, Singapore, June 23-28.
- Battistoni P., Fava G., Pavan P., Musacco A., Cecchi F., (1997). Phosphate removal in anaerobic liquors by struvite crystallization without addition of chemicals. Preliminary results. *Wat. Res.*, **31**, 2925-2929
- Battistoni P., Pavan P., Cecchi F., Mata-Alvarez J., (1998b) Effect of composition of anaerobic supernatants from an anaerobic, anoxic and oxic (A₂O) process on struvite and hydroxyapatite formation. *Ann. Chim.*, **88**, 761-772.
- Battistoni P., Pavan P., Prisciandaro, M., Cecchi F., (2000). Struvite crystallization: a feasible and reliable way to fix phosphorus in anaerobic supernatants. *Wat. Res.*, **34**, 3033-3041.
- Battistoni P., Pavan P., Prisciandaro, M., Cecchi F., (2001). Phosphorus removal from a real anaerobic supernatant by struvite crystallization. *Wat. Res.*, **35**, 2167-2178
- Battistoni P., Pavan P., Prisciandaro, M., Cecchi F., (2001b). Phosphorus removal from a real anaerobic supernatant by struvite crystallization. *Wat. Res.*, **35**, 2167-2178.
- Battistoni. P, Pezzoli S., Bolzonella D., Pavan P.,(2001a) The AF-BNR-SCP process as a way to reduce global sludge production comparison with classical approaches on a full scale basis. In: *Proc.: Spec. Conf. On Sludge Management: regulation, treatment, utilisation and disposal*. October 25-27, 2001, Acapulco, Mexico.
- Cecchi F., Battistoni P., Pavan P., Fava G., Mata-Alvarez J., (1994). Anaerobic digestion of OFMSW and BNR processes: a possible integration. Preliminary results. *Wat. Sci. Tech.*, **30**, 65-71.

- De Rooij, J.F., Heughebaert, J.C., Nancollas, G.H., (1984). A pH study of calcium phosphate seeded precipitation. *J. Coll. Int. Sci.*, **100**, 350-358.
- Eggers E., Dirkzwager A.H., Van der Honing H., (1991). Full-scale experiences with phosphate crystallization in a crystalactor. *Wat. Sci. Tech.*, **23**, 819-824.
- Joko I. (1984). Phosphorus removal from wastewater by the crystallization method. *Wat. Sci. Tech.*, **17**, 121-132.
- Kaneko S., Nakajima K., (1988). Phosphorus removal by crystallization using a granular activated magnesia clinker. *J. Water Pollut. Control Fed.*, **60**, 1239-1244
- Liberti L., Limoni N., Lopez A., Passino R., Boari G. (1986). The 10 m³/hr RIM-NUT demonstration plant at West Bari for removing and recovering N & P from wastewater. *Wat. Res.*, **20**, 735-739.
- Murakami T., Koike S., Taniguchi N., Esumi H. (1987): Influence of return flow phosphorus load on performance of the biological phosphorus removal process. In: *Biological phosphate removal from wastewaters*. Ramadori R. Ed., Pergamon Press (Oxford), 237-247.
- Nancollas, H.G. (1984): *The nucleation and growth of phosphate minerals*. In: Phosphate Minerals, Hriagn, J.O. and Moore, P.B. (Eds) Springer-Verlay
- Pöpel H. J. Jardin N. (1993). Influence of enhanced biological phosphorus removal on sludge treatment, *Wat. Sci. Tech*, **28**(1), 263-271.
- Randal C.W., Barnard J.L., Stensel H.D. (1992): Water Quality Management library Vol. 5. Design and retrofit of wastewater treatment plants for biological nutrient removal. Technomics Ed. Lancaster USA
- Salutsky M.L., Dunseth M.G., Ries K.M. Shapiro J.J. (1972), Ultimate disposal of phosphate from wastewater by recovery as fertilizer. *Effl. Wat. Treat. J.*, October 509-5019.
- Seckler, M.M., Bruinsma, O.S.L., Van Rosmalen, G.M., (1996a). Phosphate removal in a fluidised bed – I. Identification of physical processes. *Wat. Res.*, **30**, 1585-1588.
- Seckler, M.M., Bruinsma, O.S.L., Van Rosmalen, G.M., (1996b). Calcium phosphate precipitation in a fluidised bed in relation to process conditions: a black box approach. *Wat. Res.*, **30**, 1677-1685.
- Seckler, M.M., Leeuwen, M.L.J., Bruinsma, O.S.L., Van Rosmalen, G.M., (1996c). Phosphate removal in a fluidised bed – II. Process optimization. *Wat. Res.*, **30**, 1589-1596.
- Stratful I., Brett S., Scrimshaw M.B., Lester J.N. (1999). Biological phosphorus removal, its role in phosphorus recycling. *Env. Technol.*, **20**, 681-695.
- Tanaka T., Kawakami A., Yoneyama Y., Kobayashi S. (1987): *Study of the reduction of returned phosphorus from a sludge treatment process*. In: *Biological phosphate removal from wastewaters*. Ramadori R. Ed., Pergamon Press (Oxford), 201-211.